Electrical and Biomedical 4BI6

Project Thesis

Design of an Electro-ocular and Temperature sensing device for the Non-invasive Health Monitoring System (NIHMS)

by

Aiyush Bansal (0557383)

Department of Electrical and Computer Engineering
Faculty Advisor: Prof. Doyle

Electrical and Biomedical Engineering Project Report
Submitted in partial fulfillment of the requirements
for the degree of Bachelor of Engineering

McMaster University
Hamilton, Ontario, Canada
October 6, 2008

ABSTRACT

Biomedical instrumentation is a rapidly growing field where signals emanating from a human body can be analyzed non-invasively and processed. The data that is interpreted from these signals and how it is used varies from product to product. The goal of the project is to utilize these signals to give a diagnosis of the user and even offer a human-computer interface (HCI) capability. The neurons and muscles of the eye store small electrical charges within their cells. The Electro-ocular gram is a method to measure this net electrical charge between the cornea and the retina. Thus, horizontal and vertical movements of the eye correspond to a potential that can measured and correlated. Imagine an interface that lets you use a blink of an eye instead of a mouse click or a thought instead of a keystroke. What you are imagining is a neural interface. EOG is a prime example of a HCI that provides a seamless link between human and machine while increasing efficiency and productivity. By harnessing this signal, not only can the information be used for eye tracking, but also for eye diagnosis. The resting potential of the eye is proportional to the illumination of the light that it receives. Exploiting this relationship, one can diagnose the eye for diseases such as Best's disease. In addition, another signal that is acquired from the head is the temperature emanating directly from the hypothalamus, the temperature regulator in the human body. The discussion of the theory, design, and experimental results of this project will be presented.

Key words: electrooculography, EOG, human-computer interface, HCI, alternative computer input, hands-busy, assistive device, remote-monitoring, thermistor, Best's disease, Stagardt's disease, butterfly-shaped dystrophy, Biomuse, Cyberlink, macular degeneration

ACKNOWLEDGEMENTS

I would like to thank the project members in his team: Yousuf Jawahar, Mastan Kalsi, and Omer Waseem for innovative ideas, support, and perseverance. I would also like to thank the supervisor of this project, Dr. Doyle for his continued help and advice; other ECE Faculty members including Steven Spencer for supplying resistors and capacitors where needed; Dr. DeBruinn for advice; and Jerzy Smolen for supplying instrumentation amplifiers.

TABLE OF CONTENTS

ABSTRACT ii
ACKNOWLEDGEMENTS iii
LIST OF TABLES vi
LIST OF FIGURES vii
NOMENCLATURE viii
CHAPTER 1: INTRODUCTION 1
1.1: Background 1
EOG: 1
Temperature: 3
1.2: Objectives 5
1.3: Scope and Methodology 6
CHAPTER 2: LITERATURE REVIEW 8
2.1: Past Projects and Applications relating to EOG and HCI 8
EOG in eye tracking compared to other methods: 8
EOG vs. EEG: 9
Cyberlink: 11
RoboChair: 12
BioMuse: 13
2.2 Methods and Limitations in temperature measurement 14
Thermocouples vs. Thermistors vs. Infrared 15
Wireless Temporal Artery Bandage Thermometer 17
2.3 Challenges and Originality of design: 18
Originality of NIHMS 18
Challenges to face in the future 19
CHAPTER 3: STATEMENT OF PROBLEM AND METHODOLOGY OF SOLUTION 21
3.1: Theory of Calculating Core Temperature: 21
3.2: Theory of Clinical EOG and the Arden Ratio 22
CHAPTER 4: EXPERIMENTAL OR DESIGN PROCEDURES 28
4.1: Design of the Temperature system 28
4.2: Design of the EOG system 31

CHAPTER 5: RESULTS AND DISCUSSION 34
5.1: Results for Temperature 34
5.2: Results from the EOG circuit: 35
CHAPTER 6: CONCLUSIONS AND RECOMMENDATIONS 41
6.1: Project Summary 41
6.2: Statement on Project Safety 42
6.3: Challenges Faced and Recommendations for the future 43
Suggested improvements and problems with the EOG circuit: 43
Suggested Improvements and Problems with the Temperature circuit: 44
6.4: Project Cost 45
Appendix A: Matlab Code for Voltage to Temperature Conversion 46
Appendix B: Matlab Codes for Fourier and Wavelet Transforms in Processing of EOG 47
Appendix C: Complete Circuit on breadboard 49
Appendix D: Gantt Charts 50
References 51
Vita 53

LIST OF TABLES

TABLE 1. CALIBRATION RESULTS OF THE TEMPERATURE CIRCUIT VERSUS A REAL DIGITAL THERMOMETER 35
TABLE 2. TOTAL PROJECT COSTS AND COMPARISON BETWEEN MINIMUM COSTS REQUIRED AND ACTUAL COSTS PAID 45

LIST OF FIGURES

FIGURE 1. THE PHYSIOLOGY OF THE EYE [9] 1
FIGURE 2. THE ELECTRIC FIELD IN THE TISSUES SURROUNDING THE EYE AND THE EFFECT OF ROTATION OF THE EYE. [9] 1
FIGURE 3. DEMONSTRATED EOG 3
FIGURE 4. THE HYPOTHALAMUS LOCATED IN THE HUMAN BRAIN 4
FIGURE 5. A PICTURE OF THE SUPERFICIAL TEMPORAL ARTERY SHOWN ON THE LEFT SIDE OF THE HEAD 5
FIGURE 6. EYE TRACKING USING INFRARED LIGHT 8
FIGURE 7. A PICTURE SHOWING HOW INFRARED IS USED IN EYE TRACKING 9
FIGURE 8. AN EXAMPLE OF ELECTRO-RETINOGRAPHY (ERG) 10
FIGURE 9. A PERSON USING CYBERLINK TO MEASURE SIGNALS ON THE COMPUTER [3] 11
FIGURE 10. EMG-BASED HANDS-FREE WHEELCHAIR CONTROL WITH EOG ATTENTION SHIFT DETECTION, ROBOCHAIR [11] 12
FIGURE 11. MUSICAL COMPOSITIONS GENERATED BY EMG SIGNALS FROM ATAU TANAKA [6] 14
FIGURE 12. A THERMOCOUPLE SHOWN THAT GENERATES A VOLTAGE BETWEEN THE TEMPERATURE DIFFERENCE BETWEEN TWO METALS, A AND B 15
FIGURE 13. AN EXAMPLE OF A LASER THERMOMETER 16
FIGURE 14. A THERMISTOR SHOWN ON THE LEFT COMPARED TO A THERMOCOUPLE SHOWN ON THE RIGHT 17
FIGURE 15. A WIRELESS BANDAGE BASED THERMOMETER THAT IS AFFIXED TO THE STA [2] 18
FIGURE 16. CLINICAL EOG AS IT IS USED TODAY 18
FIGURE 17. DEVICE THAT THE PATIENT LOOKS AT TO PERFORM SACCADES BY LOOKING BACK AND FORTH BETWEEN THE DOTS. [3] 22
FIGURE 18. HORIZONTAL SACCADES AND THE CORRESPONDING EFFECT IN EOG 23
FIGURE 19. EOG SACCADIC AMPLITUDES IN LIGHT VS. DARK [1] 23
FIGURE 20. VERTICAL SACCADES AND THE CORRESPONDING EFFECT IN EOG 24
FIGURE 21. FIELD OF VIEW FOR THE CORRESPONDING EOG POTENTIAL USED IN EYE TRACKING. 25
FIGURE 22. A PICTURE OF BEST'S DISEASE AND THE 'EGG-YOLK' LIKE DRUSEN 26
FIGURE 23. TEMPERATURE BLOCK DIAGRAM 28
FIGURE 24. TEMPERATURE CIRCUIT VIA THERMISTOR 29
FIGURE 25. PCB DESIGN IN CADSOFT EAGLE FOR THE TEMPERATURE CIRCUIT 30
FIGURE 26. EOG BLOCK DIAGRAM 31
FIGURE 27. THE ELECTRODE THAT WILL BE USED IN THE EOG FOR NIHMS 31
FIGURE 28. EOG CIRCUIT TOPOLOGY FOR BOTH HORIZONTAL AND VERTICAL SIGNALS 32
FIGURE 29. PLOTS OF VOLTAGE VS. TEMPERATURE AND RESISTANCE VS. TEMPERATURE RESPECTIVELY IN MATLAB 34
FIGURE 30. HORIZONTAL SACCADES SHOWN ON THE HORIZONTAL OUTPUT (GREEN) AND THE VERTICAL OUTPUT (YELLOW) 35
FIGURE 31. VERTICAL SACCADES SHOWN ON THE HORIZONTAL OUTPUT (GREEN) AND THE VERTICAL OUTPUT (YELLOW) 36
FIGURE 32. RAW EOG SIGNAL (VERTICAL SACCADES) IN TIME DOMAIN 36
FIGURE 33. THE RAW EOG SIGNAL IN FREQUENCY DOMAIN. 37
FIGURE 34. THE PROCESSED EOG SIGNAL IN FREQUENCY DOMAIN 38
FIGURE 35. THE PROCESSED EOG SIGNAL IN TIME DOMAIN 38
FIGURE 36. DISCRETE WAVELET TRANSFORM OF THE EOG SIGNAL 39
FIGURE 37. INVERSE DISCRETE WAVELET TRANSFORM OF THE EOG SIGNAL 40
FIGURE 38. EOG AND TEMPERATURE COMPONENTS OF THE NIHMS PROJECT AKA THE ET BAND 41
FIGURE 39. GANTT CHART FOR 1ST SEMESTER 50
FIGURE 40. GANTT CHART FOR 2ND SEMESTER 50

NOMENCLATURE

Cones: A photoreceptor cell that functions well in high intensities of light. They are less sensitive to light than rods, but can perceive finer detail such as color and more rapid changes in images.

Core Temperature (T_c): The internal body temperature of the human body as it is regulated by the hypothalamus.

EEG: Electroencephalography, measured the potential from neural responses in the brain.

EMG: Electromyography, measures the potential of muscle activity

ERG: Electroretinography, measures the electrical impulses of the eyes with invasive electrodes.

Fixation: A fixation occurs when this movement stops, permitting the eye to acquire content.

HCI: human-computer interaction, concerns technology between the interface and communication between a human and a machine, usually a computer.

Hypothalamus: The body control center that regulates blood pressure, temperature, fluid and electrolytic balances through the process of homeostasis.

Isomerization: the process by which one molecule is transformed into another molecule which has exactly the same atoms, but the atoms are rearranged

Macula: the part of the retina that is responsible for sharp, central vision needed for reading and driving.

NIHMS: Non-invasive Health Monitoring System

Ocular Fundus: The fundus of the eye is the interior surface of the eye, opposite the lens, and includes the retina, optic disc, macula and fovea

PCB: Printed-circuit board

Photoreceptor cells: Convert light into signals that can be interpreted by the brain, consist of two types, rods and cones.

Retina: Thin layer of cells that line the back of the eye. Contains millions of photoreceptor cells that capture and convert light to electrical signals that enter the brain through the optic nerve where it is converted into images.

Retinal: an aldehyde that originates from Vitamin A that allows certain microorganisms to convert light into metabolic energy.

Rods: A photoreceptor cell that functions well in low intensities of light. It is also 100 times more sensitive to light than cones.

RPE: Retinal-pigment epithelium, pigmented layer of cells that lie underneath the retina. The RPE provides nourishment to the photoreceptors, recycles spent visual pigment, and digests the proteins of the outer segment discs which are regularly shed.

Saccade: A saccade is the fastest movement of which the human body is capable, taking only about 30 milliseconds and centers content within the foveal area.

Superficial temporal artery (STA): A major artery of the side of the head that passes in proximity to the hypothalamus.

CHAPTER 1: INTRODUCTION

1.1: Background

EOG:

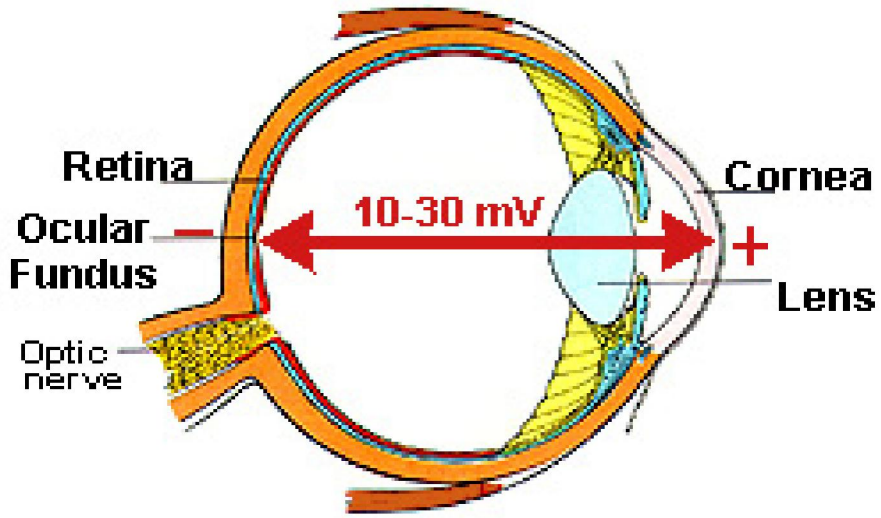

Figure 1. The Physiology of the Eye [9]

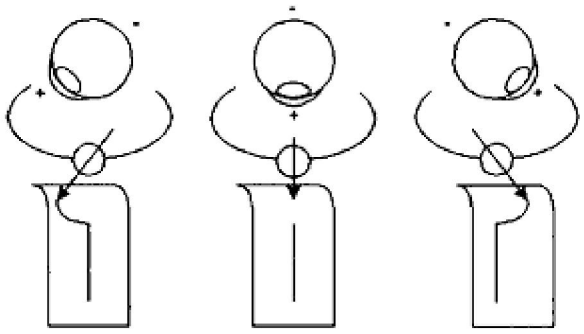

Figure 2. The electric field in the tissues surrounding the eye and the effect of rotation of the eye. [9]

Electrooculography (EOG) is a non-invasive technique for measuring the resting potential of the retina. The eye has a permanent potential difference of about 10-30 mV between the cornea and the ocular fundus, often called the cornea-fundal or cornea-retinal potential (see Figure 1). Research on general EOG states that the exact origin of the EOG has not been conclusively determined, there are many theories proposed as the mechanism behind it. The most-widely accepted is the cornea-retinal dipole theory. It states that an electric dipole is formed through the eye because the cornea is positively

charged, while the retina is negatively charged. From physics, a dipole creates an electric field that can be measured and this is the potential that is the EOG signal. This electric field in the tissues surrounding the eye changes according to the direction of the field vector because when the eye rotates, it causes a corresponding rotation of the field vector (see Figure 2). This potential gives information of the status and condition of the retinal-pigment epithelium (RPE) and it varies in response to different luminosities of light entering the retina. The function of the RPE is to provide nourishment to the photoreceptor cells through the vitamin A cycle where it isomerizes trans-retinol to 11-cis retinal. Retinal allows humans and animals to convert light into metabolic energy. Photoreceptor cells are responsible for converting this incoming light into signals that can be interpreted by the brain.

There are three known types of photoreceptor cells, but the ones that are of relevance in this paper are rods and cones. Rods are very sensitive to light, thus function well in the dark, while cones are very insensitive to light and function well in bright light, but allow perception of color and have a much faster response time to stimuli than rods. The resulting signal can be used in applications such as ophthalmological diagnosis of certain eye diseases and in recording eye movements by completing eye tracking exercises.

Typically, pairs of electrodes are placed - one above and one below the eye or to the left and right of the eye (see Figure 3). If the eye is moved from the center position towards one of the electrodes, this electrode "sees" the positive side of the retina and the other electrode "sees" the negative side of the retina. With the proper arrangement of electrodes, EOG voltages will vary proportionally with eye rotations over a range of about 30 degrees from center. Consequently, a potential difference occurs between the electrodes. Assuming that the resting potential is constant, the recorded potential is a measure of the eye position.

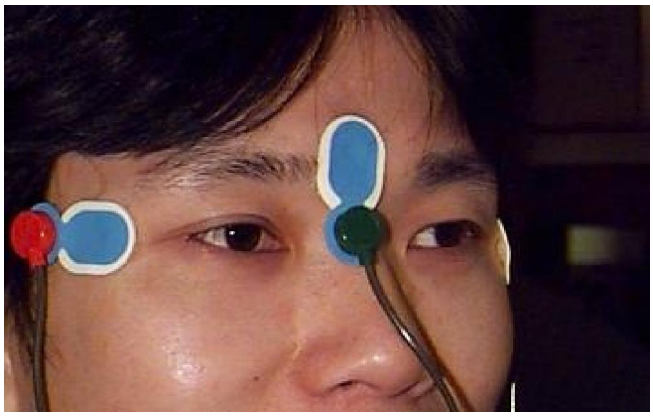

Figure 3. Demonstrated EOG[1]

Temperature:

Temperature is an important and one of the most common body signals that is monitored for health status. The hypothalamus is the control center of the body that maintains the status quo through homeostasis. Factors such as body temperature, blood pressure, fluid and electrolytic balance are maintained at a certain set-point through feedback mechanisms. The hypothalamus receives inputs from the body and compensates for any change in the environment or abnormalities (See Figure 4). For example, if it is cold outside, the hypothalamus will increase the blood pressure, pumping more blood into the body, thus increasing the core temperature. When the body is unable to maintain this balance and the temperature keeps rising in a form of positive feedback, a heat-stroke occurs. On the other hand, if the body temperature is too low, hypothermia can result.

The normal core body temperature of a health adult human being is stated to be at 98.6 degrees For 37.0 degrees Celsius. Though the human body temperature can still vary due to an individual's metabolism rate – the higher (faster) it is, the higher the normal body temperature and the slower the metabolic rate the lower the normal body temperature. Other factors that might affect the body temperature of an individual may be the time of day or the part of the body in which the temperature is measured at. The body

[1] http://www.univie.ac.at/cga/courses/BE513/Projects/

temperature is lower in the morning, due to the relaxed state of the body and higher at night after a day of muscular activity and after food intake.

Body temperature also varies at different parts of the body. Oral temperature, which is the most convenient type of temperature measurement, is at 37.0 °C. This is the accepted standard temperature for the normal core body temperature. Other measurements are external and are taken in the armpit or between two folds of skin on the body using a thermometer. This is the longest and most inaccurate way of measuring body temperature, the normal temperature falls at 97.6 °F or 36.4 °C.

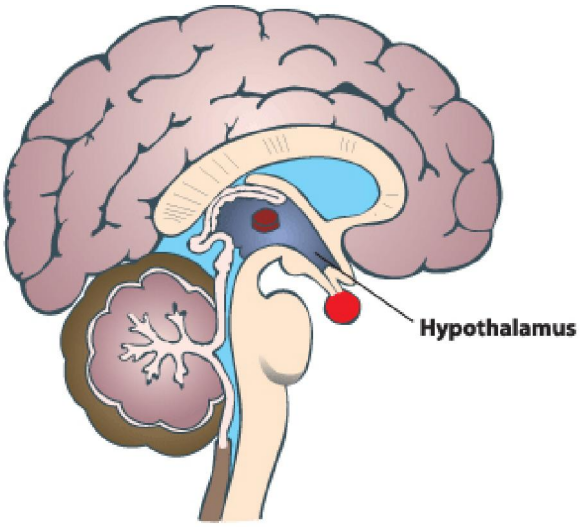

Figure 4. The Hypothalamus located in the human brain[2]

Rectal temperatures are an internal measurement taken in the rectum, which fall at 99.6 °F or 37.6 °C. It is one of the most accurate and least time consuming types of body temperature measurement, being an internal measurement. However, it is not the most comfortable method to measure the body temperature of an individual.

Therefore, another way to measure the core body temperature is possible through the superficial temporal artery (STA), an artery that passes in proximity to the hypothalamus, resulting in a very accurate way of assessing the core body temperature because the

[2] https://eapbiofield.wikispaces.com/file/view/Hypothalamus.jpg

hypothalamus is the temperature regulator of the body. This artery lies close to the skin surface in the temple region of the forehead. The temporal artery behaves as a heat source maintained at a core temperature, T_c. In addition, the STA branches off the carotid artery supplying the brain, the blood flow remains fairly constant and thus the temperature is also constant and near T_c (see Figure 5) .

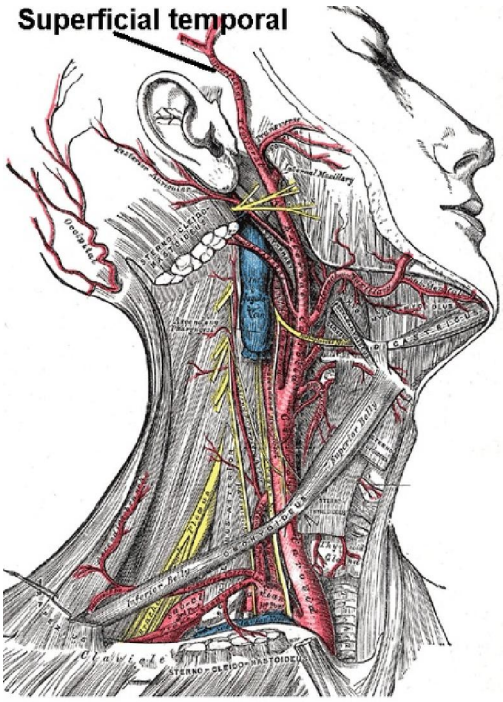

Figure 5. A picture of the superficial temporal artery shown on the left side of the head[3]

1.2: Objectives

The objective of this project is to utilize a method that doctors, family members, or the user, can monitor signals emanating from the body that diagnose health. The name of the project is "Non-Invasive Health Monitoring System" (NIHMS). Its purpose is to establish a device that is portable, wireless, real-time, wearable, non-invasive, and as comfortable as possible. NIHMS consists of four different transducers that monitor blood pressure, breathing rate, oxygen saturation, pulse rate, EOG, and temperature. All of these signals are sent wirelessly to a smart phone, PDA, or other capable device in which a person can look at the information and the prognosis of that information.

---

[3] http://upload.wikimedia.org/wikipedia/commons/a/a2/Superficial_temporal_artery.PNG

This system gives users the freedom of mobility while still continuously monitor themselves instead of lying on a bed in a hospital connected to many different devices. The target audience for NIHMS are people who are severely disabled, paralyzed, or in a condition where they need to be monitored extensively. While there are certain cases where paralysis destroys mobility, NIHMS provides an alternative HCI approach for those users through EOG, especially neuro-muscular diseases. The data can also be recorded showing doctors past results as well as present, so a comparative analysis can be done between normal and abnormal. NIHMS not only supplies the results, but can process the results to alert the user of any possible warnings and send a signal wirelessly to a doctor or any emergency help. There are many patients in the world who die because of the response time between medical care and the time when body signals are interpreted to be in danger. A real-time monitoring system reduces this response time considerably. Now babies in the hospital can be monitored continuously while doctors and nurses can concentrate on other patients with higher priority. Also, patients who thought they would have to live their whole life in a hospital now have an opportunity to do something more.

While the target audience is relatively small, this product can also be used for the average human being who wishes to stay healthy or monitor themselves during a rigorous exercise. Just as a person carries accessories such as a watch, cellphone, music player, etc. – all of these devices provide information that the user can use. Providing a solution that can be accessorized and provide even more information, NIHMS has application to all people.

1.3: Scope and Methodology

The scope of this particular project will deal with two of the transducers of the NIHMS device, namely temperature and EOG. This paper will not discuss the design and methodology of the other two transducers nor the wireless transmission via a Bluetooth device. The software required to process the signals, however, will be discussed and shown how to implement. The final product presented in this paper is a prototype of the complete product.

Therefore, the methodology of this project consists of two separate devices, one for measuring temperature and one for EOG. The hardware design for both of these will be discussed and implemented. Furthermore, the output of these hardware devices will generate a voltage range in which the microcontroller can read. After the micro-controller, these signals can then be sent to LabView, a graphical user-interface that can process the signals in real-time or to Matlab for post-processing. Both techniques were done for proof of concept. Matlab will be used in the prototype to emphasize more detail on the processing techniques.

For the temperature measurement, a thermistor is used to measure the body temperature from the superficial temporal artery to give as accurate of a temperature as possible. An elastic headband will be used that the user can wear, inside will be the circuitry for the temperature measurement such that it overlaps the area where the STA is located. The area where the circuitry is located will be insulated from the outside material, but the inside will use aluminum to act as a conductor for the thermistor.

For the EOG, horizontal and vertical saccadic movements of the eye will be recorded in light and dark adaptation. Saccades are fast movements of the eye when the eye jumps from one point to another. Theory suggests that the maximum amplitude in the light over the minimum amplitude in the dark, give a diagnosis known as the Arden Ratio. The data collected during the light and dark adaptation will allow calibration of the device, which after, a diagnosis should be possible continuously in any illumination of light. Thus, the results and diagnosis of the temperature and EOG will be shown.

The final device will be an elastic headband that the user can wear and is able to do send EOG and temperature signals to a Bluetooth transmitter.

CHAPTER 2: LITERATURE REVIEW

2.1: Past Projects and Applications relating to EOG and HCI

EOG in eye tracking compared to other methods:

The most popular accomplished neural-interface with the EOG would be the EOG-controlled mouse. Here EOG provides the direction of the mouse according to the eye movements and an EMG signal measures the muscle activity in the eye corresponding to clicking of the mouse. Even for non-physically impaired people, such a device allows a user to move a cursor without having to lift the hand from the keyboard. This type of technology is already helping users that have severe disabilities. Especially victims of paralysis and debilitating muscular diseases such as amyotrophic lateral sclerosis, the standard keyboard-mouse interface does not work.

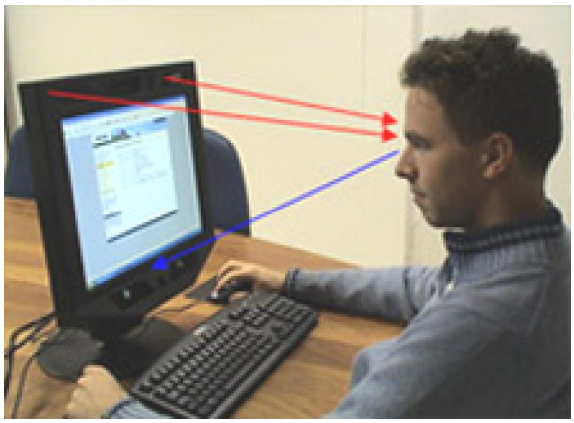

Figure 6. Eye tracking using infrared light[4]

Other methods used to for tracking a person's gaze include optical cameras and infrared beams. This works when the infrared light is transmitted to the eye to illuminate the eyes, a CCD (Charged Couple Device) sensor then captures the reflected light from the eyes (See Figure 6). When a fixed light source is directed at the eye, the amount of light reflected back to the CCD will vary with the eye's position (see Figure 7). Infra-red light

[4] http://www.uxmatters.com/mt/archives/2005/12/introduction-to-eyetracking-seeing-through-your-users-eyes.php

is also ‘invisible’ to the eye, so it does not distract the user in any way. Also, since infrared light is not influenced too much by other light sources, the illumination from the environment does not affect measurements. EOG, however, is much less costly alternative, allowing the target audience to use the product more. Blinks can also be a problem, as the eyelids cover the surface of the eye, altering the amount of light reflected for a short time after the blink. The eye tracking done with EOG has gone to the extent where Stanford University is using a way to develop to adjust fiber-optic cameras during endoscopic surgery such that the cameras synchronize with the EOG signals of the surgeon. This not only allows the doctor control of the view of the place where he or she is operating, but also allows the doctor to use other tools because their hands will be occupied while their eyes can move the camera.

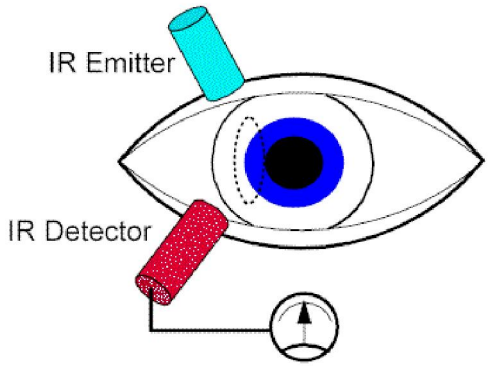

Figure 7. A picture showing how infrared is used in eye tracking[5]

EOG vs. EEG:

EOG has almost always been paired with EEG in most projects, but EEG is too complex to completely filter the noise since the brain varies from person to person, the calibration is very difficult and even more difficult to process. One of the signals that EEG can detect, the rapid-eye movement (REM) can also be detected by EOG during a sleep state. Most attempts to establish a HCI using EEG work by monitoring alpha and mu waves because these waves change with emotion. However, this is a laborious process for a person to learn to control with their emotions. Although, there has been some application

[5] http://www.liv.ac.uk/~pcknox/teaching/Eymovs/emeth.htm

for people who are in coma and in this case, cannot move their eyes either. With fully body paralysis, only brain waves can be monitored – some devices were able to employ an "alpha-wave switch", which could output yes or no for a question. Devices such as these have actually been successful, but it takes many iterations of "yes's" and "no's" to narrow down to a single answer. [6]

Another EEG implementation used evoked potentials (EP). In particular, Erich E. Sutter Research Institute in San Francisco developed a system that allows handicapped people to select words or phrases from a flashing menu by keeping their gaze fixed on the desired word for more than two seconds. The machine can monitor the form and timing of the EP response and can discriminate between which flash caused the EP. [6]

EOG vs. ERG vs. VEP

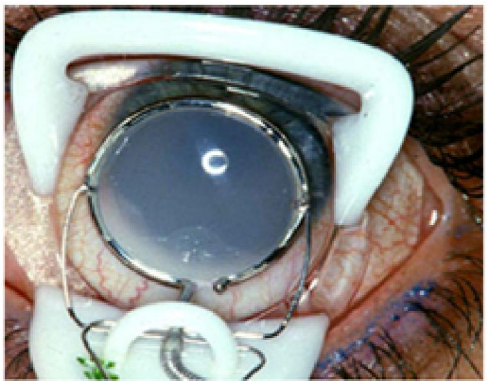

Figure 8. An example of Electro-retinography (ERG)[6]

There are other methods used in the clinical world that take measurements from the eye and are able to do diagnosis on them as well. One method is called ERG (Electro-retinography), where electrodes are placed on the eye invasively and measure the electrical activity of the retina in response to light (see Figure 8. An example of Electro-retinography (ERG). Ophthalmologists use ERG to diagnose various retinal diseases. The problem with this method is that it is extremely

[6] http://webvision.umh.es/webvision/imageswv/DONFig4.jpg

invasive and not practical. Therefore, EOG serves as an alternative to diagnose a small amount of diseases, but is the only approved method to diagnose a disease called Best's disease.

Visually evoked potentials (VEP) are also used; it is caused by sensory stimulation of a subject's visual field and is observed using EEG. The visual stimuli used usually are flashing lights or checkerboards which flicker back and forth. VEPs are useful in detecting blindness in people who are not able to communicate effectively such as babies or animals. When there are delays to visual stimuli, this could mean that multiple sclerosis might be present. There are disadvantages of this method due to the different stimuli present and the wide variety of the responses from different people. This correlation is difficult to perceive in an EEG. Also, if the hardware circuitry to receive these signals is not properly calibrated, then it could result in a mis-diagnosis.

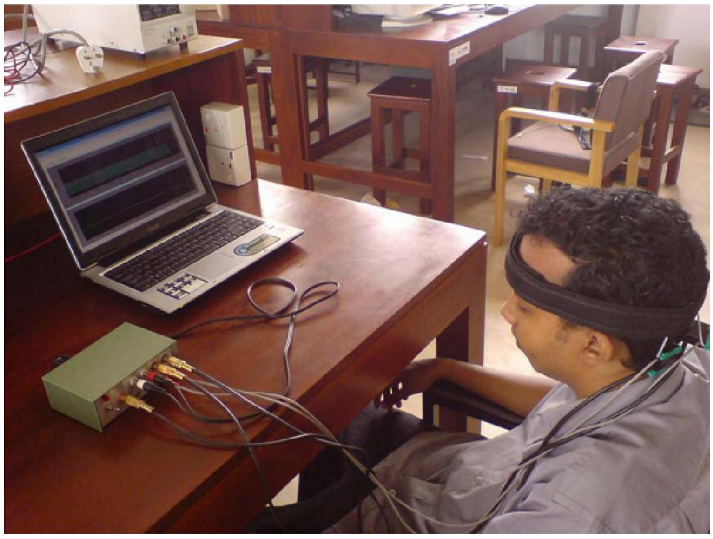

Figure 9. A person using Cyberlink to measure signals on the computer [3]

Cyberlink:

The Cyberlink (Figure 9) is a product most similar to the final product of this paper. It uses a headband that the user can wear and monitor EOG, EEG, and EMG altogether. The NIHMS project also uses a headband, but integrates EOG and temperature with the application of diagnosis. This allows a wearable and comfortable solution for the user. This done through AgCl electrodes embedded within the cloth of the headband. In

addition, Cyberlink separates brain activity into 10 different frequencies called "Brainfingers". If these Brainfingers could be harnessed correctly without noise of other thought processes, it could be mapped to functions most accessible by the user such as the opening of a program, selection of a function within a program, etc. Even without EEG, Cyberlink uses eye and muscle movements to generate a digital signal that is sent to a 12-bit analogue-to-digital converter (ADC), where a small microcontroller is able to translate these signals appropriately to keystrokes and mouse commands. Cyberlink was originally developed for video game interface by Andrew Junker of Brain Actuated Technologies in 1998. [1]

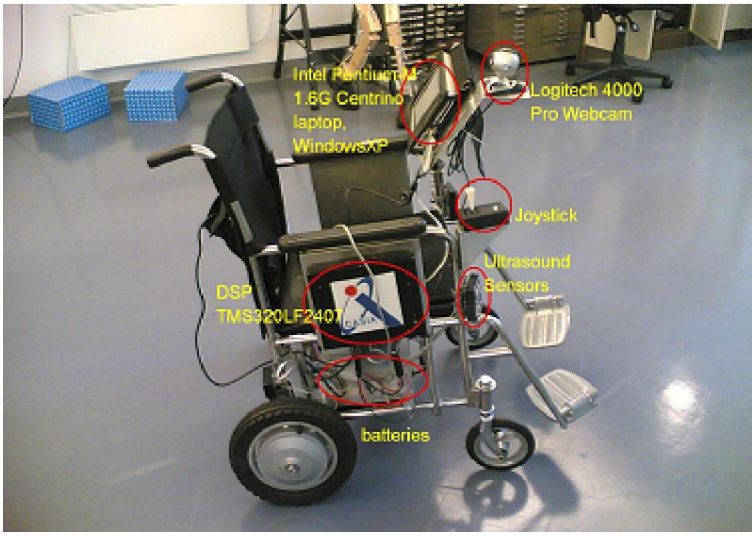

Figure 10. EMG-based Hands-Free Wheelchair Control with EOG Attention Shift Detection, RoboChair [11]

RoboChair:

Most electrically powered wheelchairs are controlled by a joystick, but this does not satisfy the needs for users who have restricted limb movements caused by diseases such as Parkinson's disease and quadriplegics. There have been many solutions proposed such as voice recognition, EOG eye tracking control, and vision based head gesture control. Although EOG eye tracking and head gesture control work, users are not normally looking around their environment for safety reasons such as unwanted movements. The RoboChair is a hands-free control system in which the EMG is used as a directional control while EOG is used as a speed control (see Figure 10). To do this, the RoboChair

employs the use of the “Cyberlink” discussed above. To avoid non-voluntary movements, the RoboChair has a switch between the “control” state and the “non-control” state. This way, the user is able to still use facial expressions and head gestures during the non-control state and avoid unnecessary movements that could result in collisions. For even more safety buffer, the RoboChair uses 6 ultrasonic range sensors for obstacle avoidance. The RoboChair is low cost, easy to setup and use. A new user requires practice with the simulator for about half an hour before having mastered the system. This can be the same for new computer users who have never used a mouse before. [11]

BioMuse:

In 1992, Benjamin Knapp and Hugh Lusted of BioControl Systems at Stanford University developed the BioMuse, a high-end biocontroller that utilizes EMG and EEG signals. The unique attribute of the BioMuse compared to the previous devices, is that it can convert these signals into a sound signal, particularly MIDI. The electrodes are attached to the arms of the user to pick up neural and muscular activity (see Figure 11). Later, a man named Atau Tanaka, who studied electronic music at Harvard University, was the first person to actually compose music for the BioMuse. After one year, Atau Tanaka, Zbigniew Karkowski, and Edwin van der Heide used the Sensorband, in which each person uses the body to make music, forming a band. Tanaka played the BioMuse; Karkowski played an invisible cage of infrared beams that, when broken, trigger a sample of sounds; and Van der Heide played a MIDI conductor using joystick-like controls. This was the first long-distance electronically created music band.

Figure 11. Musical compositions generated by EMG signals from Atau Tanaka [6]

2.2 Methods and Limitations in temperature measurement

There are many different methods of measuring body temperature such as thermocouples, thermistors, and IR receivers. The advantages and disadvantages of these methods in comparison to one another will be discussed below. Clinically and at home, most of these thermometers have to be manually controlled (someone needs to hold them). For babies and children, this can be troublesome and an accurate temperature reading cannot be acquired unless an adult is to interfere. However, the temperature measured on the forehead via a headband, allows babies to be monitored continuously without heavy interference. Accuracy is a very important factor in temperature measurement and this is why other products have aimed at measuring the core body temperature using the STA. An example of a product that will discuss is called the Wireless Temporal Artery Bandage Thermometer which will utilize the measurement at the STA.

Thermocouples vs. Thermistors vs. Infrared

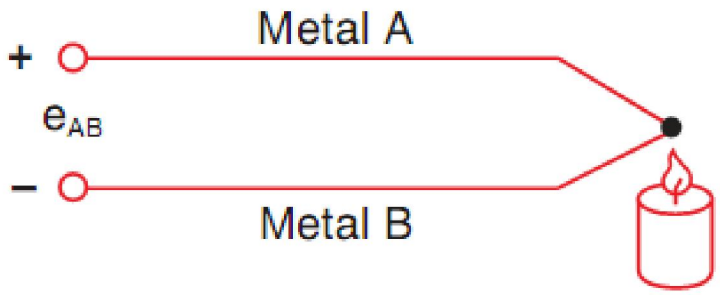

Figure 12. A thermocouple shown that generates a voltage between the temperature difference between two metals, A and B. [11]

Thermocouples are among the easiest temperature sensors to use and obtain and are widely used in industries. Thermocouples are pairs of dissimilar metal wires joined at least at one end, which generate a net voltage between the pair according to the magnitude of the temperature difference between the two ends (see Figure 12). Thermocouples are known for their very large temperature range (0 to 1100° C). However, the range of interest for human body temperature is only 20 to 45° C. The disadvantage of thermocouples is that they are not very accurate and have errors around +-2 ° C. Furthermore, since it measures a voltage based on the difference of two metals, a reference temperature is needed for one of those metals. This poses a problem because the environment has a variable temperature, so it cannot use this as a reference. Also, only the core body temperature is of interest and not just a surface temperature with respect to an outside temperature.

Figure 13. An example of a laser thermometer[7]

Another method used, infrared sensors work by measuring infrared radiation emitted from the body. The advantage of these types of thermometers is that they can show the temperature at many locations on the body instead of just a fixed point. For example, laser thermometers can shine laser light on the point of the body where the measurement is desired or non-contact thermometers can measure the temperature from a distance without ever touching the body (see Figure 13). By knowing the amount of infrared energy emitted by the object and its emissivity, the object's temperature can be determined. The design uses a lens to focus the infrared energy on to a detector, which converts the energy into an electrical signal which can be displayed in units of temperature. Clinicians then have the advantage of facilitating temperature measurement without contact to the patient. As such, the infrared thermometer is useful for measuring temperature under circumstances where thermocouples or other probe type sensors cannot be used. In terms of accuracy, infrared thermometers exceed thermocouples. The disadvantage is that infrared thermometers are very expensive and the design of the detectors that receive radiation can be cumbersome. Therefore, the last alternative is thermistors.

[7] http://www.sale-tag.com/images/1197794460822-1996385766.jpeg

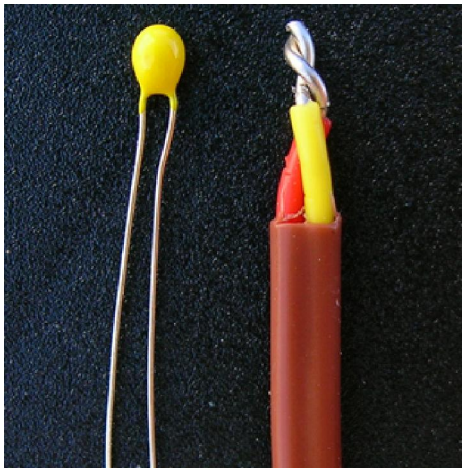

Figure 14. A thermistor shown on the left compared to a thermocouple shown on the right[8]

Thermistors are most accurate and inexpensive temperature sensors available, offering an inaccuracy of less than 1%, that is +-0.1° C. Since the region of interest is STA, a thermometer that is capable of measuring in different parts of the body such as the infrared thermometer is not necessary. The size of thermistors is also very small, allowing wearability (see Figure 14). The only disadvantage of thermistors is that they have a very small operating range, but for measuring human body temperature, this is just perfect (20 to 40° C). If the core temperature is outside this range, then the user is already in need of medical care and the diagnostic system give a warning. Thermistors can be classified in two types – PTC (positive-temperature coefficient) and NTC (negative-temperature coefficient). For example, if the resistance decreases as the temperature increases, it is NTC and vice versa.

Wireless Temporal Artery Bandage Thermometer

This product is very similar to NIHMS as it employs the use of thermistors to measure the core body temperature from the STA. There are two arrays of four thermistors is placed along the length of the bandage, one to measure the temperature of the skin, and one to measure the temperature of the bandage. Using Fourier's law of heat conduction is

[8] http://www.apogee-inst.com/images/thermistor_thermocouple.jpg

then used to calculate the core temperature by relating the flux density flowing out of the skin to the heat loss from the STA. It also has a 2.4 GHz RF transceiver that can transmit the signal wirelessly (see Figure 15).

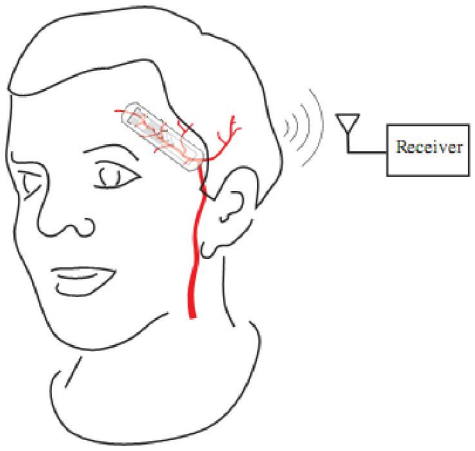

Figure 15. A wireless bandage based thermometer that is affixed to the STA [2]

2.3 Challenges and Originality of design:

Originality of NIHMS

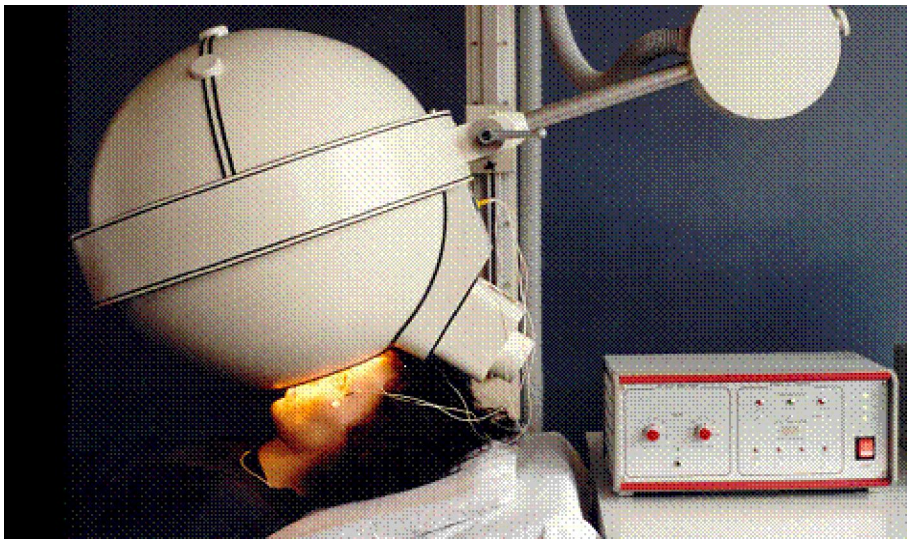

Figure 16. Clinical EOG as it is used today[9]

[9] http://neurophysiologyindia.com/potentials.htm

NIHMS tries to simulate the clinical procedure for EOG diagnosis shown in Figure 16 in a portable and wireless solution instead of the current enormous device that exists ttoday. NIHMS incorporates some aspects from both the Cyberlink and the Wireless Temporal Artery Bandage Thermometer into one minimized device. The unique ability of NIHMS is that it offers the choice of HCI along with diagnostic information from the signals. The disadvantage of the bandage thermometer was it used two arrays of four thermistors. NIHMS tries to minimize the design as much as possible so it is accurate enough for measurement and small enough to be comfortable. NIHMS uses only one thermistor and calibrates with other thermometers for ease of design. The temperature circuit is embedded within the headband that measures EOG as well. Many of the devices discussed above also used Cyberlink as the measurement device, but put their own different applications of it. In this case, NIHMS has its own hardware design for the measurement device and its own software for the processing.

Challenges to face in the future

Challenges faced by individuals in the past were mostly noise; specifically motion artifact since movements of the body causes movements of wires, which in turn causes a capacitance to develop between the wires. For example, the computer mouse would move sometimes in a direction not desired by the user because the user might have moved his head slightly. This can be avoided by using a wireless topology. However, there are still problems with electromagnetic interference that is encountered since the human body acts like an antenna. These interferences need post-processing to be completely filtered. Also, a wireless topology also adds another source of noise at the receiver end of the transmission.

Another problem is delay; all digital components have some form of delay, so the neural-interface established is still too slow for able-bodied people to use effectively. The time between when a user thinks of something to do and the response of the machine to do that action needs to be minimized. Sampling rate also needs to be very high as to avoid quantization problems in the received signal.

Extensive studies have been done on the brain, but there is not enough information to completely model a brain. People have not been able to identify the underlying patterns from the fluctuations in voltage on a person's scalp. There has been little success in mapping these signals by function, for example, which set of brain waves will arise when a person thinks of an alphabet

These are some of the reasons why neural-interfaces have not yet been realized into society, but the research is still in its infancy. The advances of the next century might allow realization of thought-recognition systems in the future.

CHAPTER 3: STATEMENT OF PROBLEM AND METHODOLOGY OF SOLUTION

3.1: Theory of Calculating Core Temperature:

The design of the temperature circuit starts with the transducer, the thermistor. The thermistor resistance changes according to: $R = R_o \exp\left[\beta\left(\frac{1}{T} - \frac{1}{T_o}\right)\right]$ where R_o is the resistance at T_o. Through this equation, the resistance can be calculated based on temperature changes on the skin surface of the forehead. Then after some hardware circuitry, a voltage to resistance relationship will be established. The core temperature can be calculated based on Fourier's law of heat conduction, the heat flux flowing out of the skin, q_{skin} [W/m^2], due to heat loss from the temporal artery can be calculated from: $q_{skin} = h_{tissue}(T_c - T_s)$ where T_s is the temperature of the skin and h_{tissue} is the heat transfer coefficient that depends on tissue thickness, tissue composition, and the level of perfusion. The heat flowing from the skin is equal to the heat lost to the environment: $q_{env} = h_{env}(T_s - T_{env})$. In this case, there is an insulator between the temperature circuit and the environment within the headband. This means this insulator is where the heat loss from the skin is transferred to instead of the environment i.e. $q_{env}=q_{ins}$. Equating the heat from the skin to the heat in the insulator leads to: $h_{tissue}(T_c - T_s) = h_{ins}(T_s - T_{ins})$ and solving for T_c, results in: $Tc = \frac{h_{ins}}{h_{tissue}}(T_s - T_{ins}) + T_s$. Measuring Ts and Tins with thermistors within the headband, the device can be calibrated so that $\frac{h_{ins}}{h_{tissue}}$ gives an accurate T_c. However, there were many assumptions made – first, the heat transfer coefficients vary based on many factors such as airflow and perfusion, but the ratio of these is fairly constant; second, perspiration can add a lot of error since the heat loss due to evaporation is neglected. For this prototype, the skin temperature will be assumed to be at the same temperature as the insulator i.e. $T_s=T_{ins}$, which leads to the core temperature is equal to the skin temperature. This does not yield accurate results, but this is only for the prototype.

3.2: Theory of Clinical EOG and the Arden Ratio

In the real world, the clinical EOG system that is used have standards that are determined by the ICSEV (International Society for Clinical Electrophysiology and Vision). As discussed before, the EOG signal changes in response to retinal illumination. In particular, the EOG signal decreases for 8-10 minutes in the dark and subsequent illumination in the light causes an initial drop for the first 60 – 75 seconds, but rises again for 7-14 minutes (see Figure 19). The standard procedure recommended by ICSEV begins with the patient in the pre-adaption phase. In this phase, the patient should not be exposed to any large changes in illumination (light/dark). Afterwards, the patient is placed in front of a device called the Ganzfield that shows 3 dots evenly spaced from each other. This is shown in Figure 17, where the red dot represents the center of field vision.

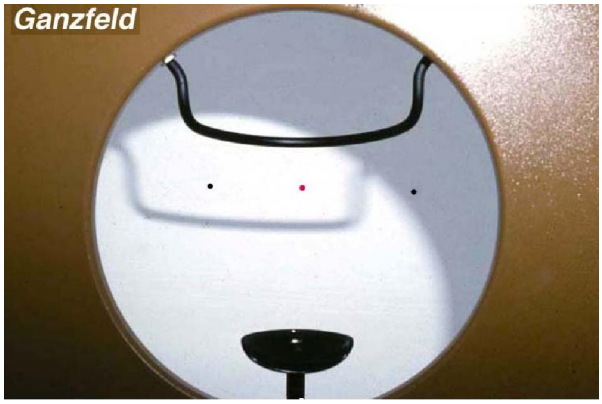

Figure 17. Device that the patient looks at to perform saccades by looking back and forth between the dots. [3]

The patient is then asked to move his eyes from left to right to record the horizontal saccades for 15 minutes in the dark. The result of the EOG is shown in Figure 18; as the eyes move towards the electrodes, the EOG potential rises and as it is moved away, the potential decreases. Afterwards, more horizontal saccades are recorded for another 15 minutes in the light phase.

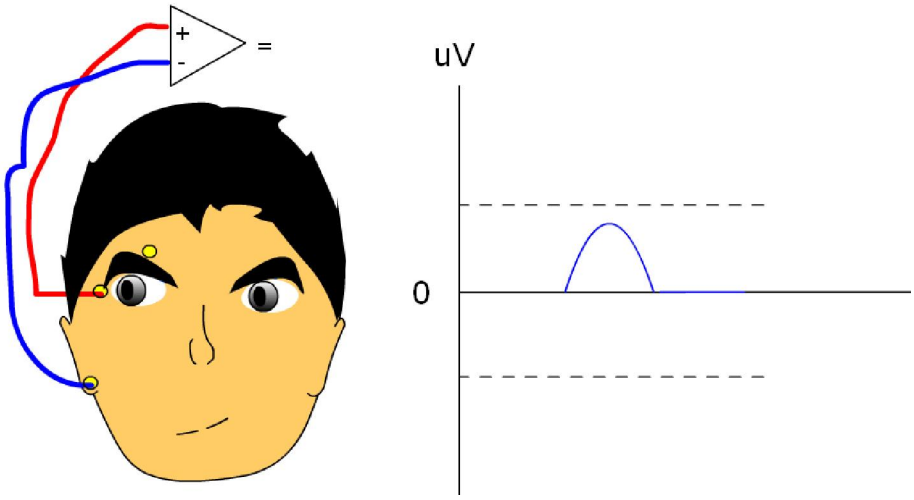

Figure 18. Horizontal Saccades and the corresponding effect in EOG

After 30 minutes of data collecting in the dark and light phases, the Arden Ratio can then be computed by taking the ratio of the maximum amplitude in the light (Light peak, Lp) over the minimum amplitude in the dark (Dark trough, Dt). An example of how the data looks is shown in Figure 19. This shows how the EOG amplitudes change with illumination and the initial drop during the transition from dark phase to light phase.

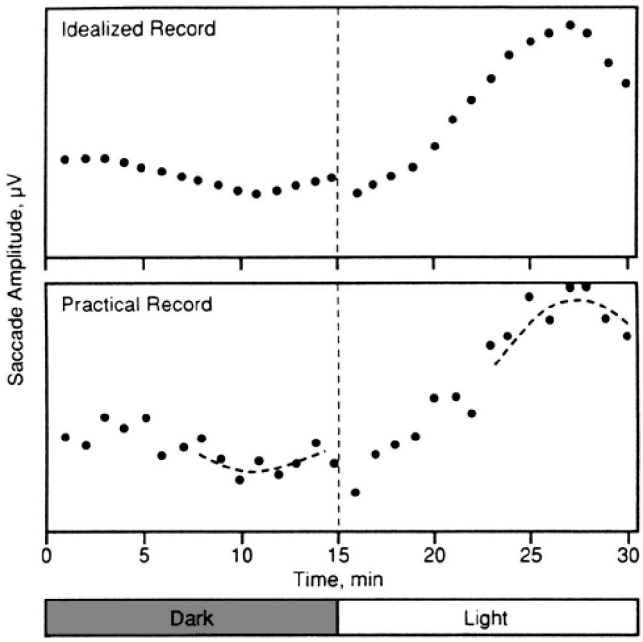

Figure 19. EOG Saccadic Amplitudes in Light vs. Dark [1]

There are two methods accepted by the ICSEV for the Arden Ratio:

Method 1: $Arden\ Ratio = \left| \frac{Lp}{Dt} = \frac{Light\ peak}{Dark\ trough} \right| * 100$ $abnormal\ EOG < 150\%$ **Method 2:** $\frac{Lp}{Db} = \frac{Light\ peak}{Dark\ baseline} * 100$

In Method 1, the Lp/Dt ratio is taken where if below 1.5, it indicates an abnormal EOG and further tests need to be conducted to assess the status. This method is used for an initial calibration of NIHMS. Once Method 1 is established for one person, a correlation can be done between Method 1 and Method 2. In Method 2, the Lp/Db is taken where Db is the dark baseline or the minimum amplitude in the current illumination setting. Method 2 is what allows NIHMS to monitor the EOG continuously and still do the diagnosis. This way the patient can be outside in the day, where the illumination is bright and still do the diagnosis without reverting to the dark phase.

In the standard clinical procedure, only horizontal saccades are taken into account. For this project, both horizontal and vertical saccades will be considered. Therefore, after recording the horizontal saccades, the same procedure must be repeated for vertical saccades. The patient will be asked to move his eyes up and down, creating an EOG that rises when the eyes move up (towards the electrode) and decreases when the eyes move down (away from the electrode). An example of the effect is shown in Figure 20.

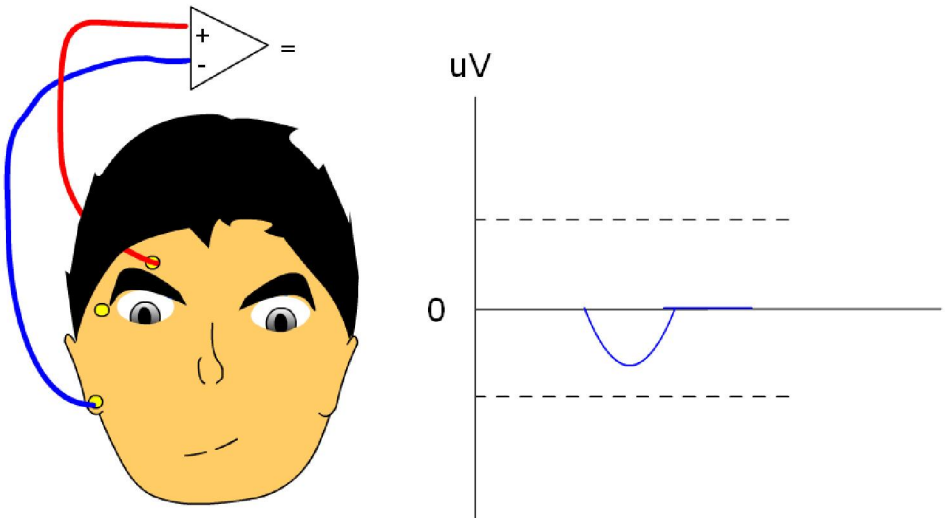

Figure 20. Vertical Saccades and the corresponding effect in EOG

Since both horizontal and vertical saccades will be considered, there will be a corresponding Arden ratio associated with each. Therefore, the magnitude of the horizontal and vertical Arden ratios is what will be used to determine the diagnosis: $Arden\,Ratio\,Magnitude = \sqrt{(Vertical\ AR)^2 + (Horizontal\ AR)^2}$. Similarly, the LP/Db can be computed as: $Lp/Db\,Magnitude = \sqrt{(Horizontal\ LP/BL)^2 + (Vertical\ LP/BL)^2}$. Since the Db > Dt, the Lp/Db ratio will be lower than the Arden Ratio. The difference between these two ratios will be an offset that will be used for calibration of the device. Once this offset is known, the user no longer has to re-calibrate the device.

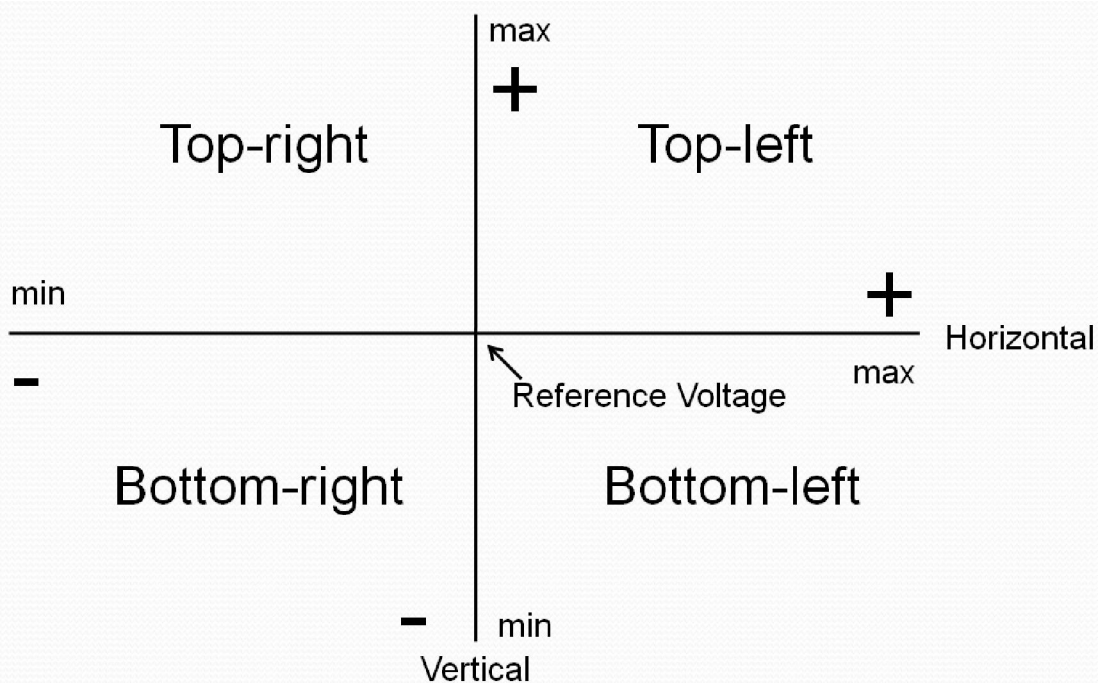

Figure 21. Field of View for the corresponding EOG potential used in eye tracking.

To implement HCI, Figure 21 is used to map the corresponding vertical and horizontal signals from the EOG. When the user is looking straight head in the center, this constitutes as the origin and the voltage during this time for the horizontal and vertical signals will serve as a reference voltage for each. When the horizontal signal is positive, this means the user is looking towards the electrode, which will be in the left direction and vice versa. In addition, when the vertical signal is positive, the user is looking up. This way, eye tracking can be achieved.

3.3: Diseases that are diagnosed by EOG

Macular degeneration, sometimes called AMD (Age-related macular degeneration), is the leading cause of vision loss and blindness for people above the age 65. The macula is a light-sensitive tissue, located at the center of the retina, which is responsible for the sharp, central vision needed to read or drive. There are two forms of macular degeneration, wet and dry. Wet AMD occurs when there is an abnormal growth of blood vessels under the macula. These new blood vessels are very fragile and therefore, break and leak blood into the macula, causing the macula to rise above from its normal place. A symptom of Wet AMD is when straight lines begin to appear wavy. Dry AMD occurs when the tissues around the macula start to deteriorate and leaking material, causing yellowish spots known as 'drusen' to appear. A symptom of Dry AMD is a blind spot in the center of vision.

Figure 22. A picture of Best's disease and the 'egg-yolk' like drusen[10]

Some of these diseases affect juveniles (JMD – Juvenile Macular Degeneration) and are caused by genetic factors. These genetic factors are caused by mutations in genes that disrupt Vitamin A cycle and cause retinol to not properly be used as previously discussed in Chapter 1. Stagardt's disease, the most common JMD and Best's disease, the second most common JMD are both examples of this (see Figure 22). EOG is able to diagnose both of these diseases and is known for diagnosing Best's disease. All of these diseases have different stages and if not diagnosed at an early stage, could lead to major problems.

[10] http://webvision.umh.es/webvision/imageswv/DONFig50.jpg

The advantage of EOG is that if Best's disease is present, the EOG is abnormal regardless of the stage of the disease.

CHAPTER 4: EXPERIMENTAL OR DESIGN PROCEDURES

4.1: Design of the Temperature system

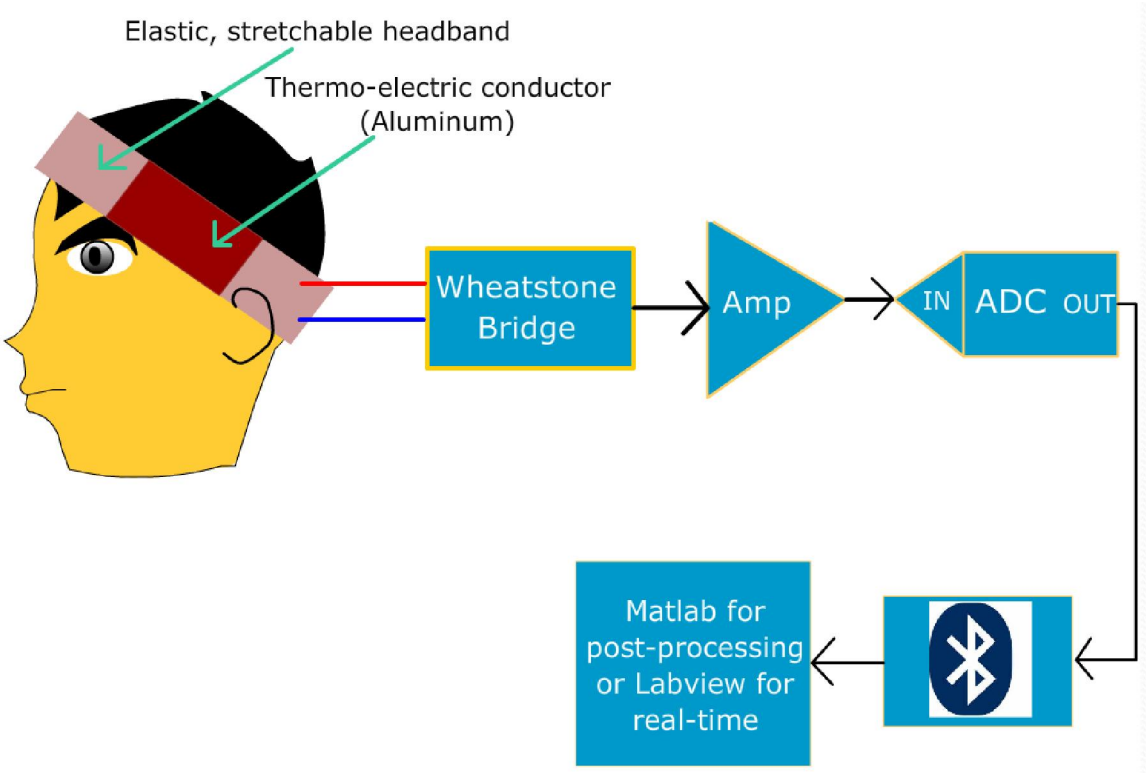

Figure 23. Temperature Block diagram

The design of the temperature circuit starts with the headband. The darker red area shown in Figure 23 is where the temperature circuit is embedded. The interface between the skin and the circuit is a conductor, for this design, aluminum while the interface between the circuit and the environment is an insulator, nylon in this case. The remaining part of the headband can either be elastic or an adjustable belt-like strap that can conform to any head size. The aluminum will cover the thermistor so that the conduction of heat flux from the skin can be received by the thermistor. To measure the resistance of the thermistor, a wheatstone bridge circuit is used. Then to convert this reading into a voltage with respect to a node in the wheatstone bridge, it is followed by a differential amplifier. This voltage is inputted into the ADC of the microcontroller. This is then transmitted via Bluetooth wirelessly to a processor or computer. For real-time processing, LabView is used while for post-processing Matlab can be used to calculate the temperature based on the voltage signal received.

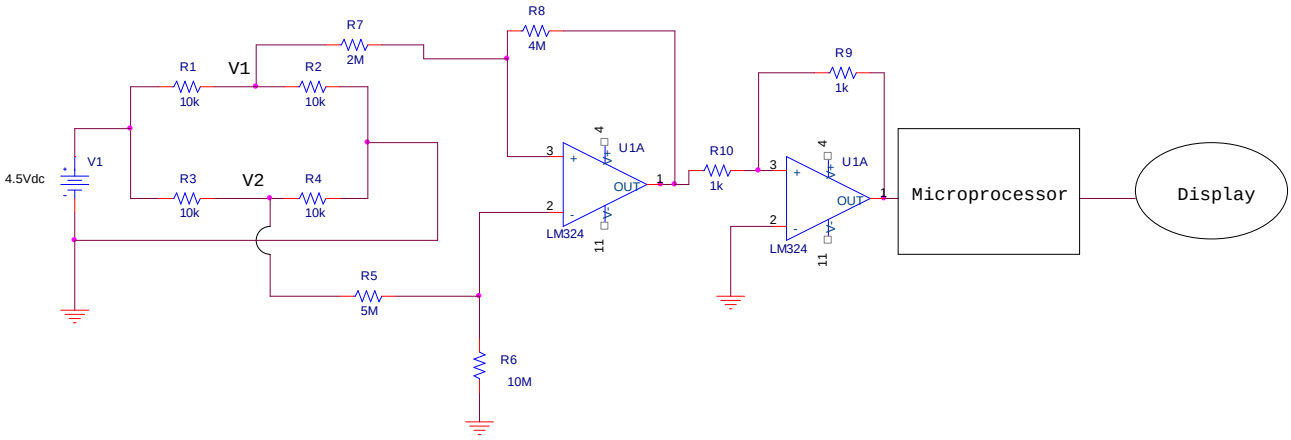

Figure 24. Temperature circuit via thermistor

The exact circuit topology is shown in Figure 24. The power supply is 4.5 V which is fed into the wheatstone bridge of the four resistors R1-R4 where R1 is the variable thermistor. To stabilize the wheatstone bridge, R4 was initially set as a potentiometer and an ammeter was used to assess the current flowing between nodes V1 and V2. The potentiometer is varied until the current in the ammeter is zero. In this project, R4 was found to be 10kohms. Then the differential signal from nodes V_1 & V_2 are fed into a differential amplifier with a gain of 2. This is followed by an inverting amplifier with a gain of -1, this is to ensure that the input signal range to the microcontroller is between 0 to 5 V for the temperature range of interest (25-50°C). The output of this can then be transmitted wirelessly and processed. The calculations for the circuit in Figure 24 are shown below:

$$V_1\left[\frac{1}{R_2}+\frac{1}{R_1}\right]-V_s\frac{1}{R_t}=0$$

$$V_1=V_s\frac{1}{R_t}\left[R_t \parallel R_1\right]$$

$$V_1=Vs\left[\frac{R_1}{R_1+R_t}\right]$$

$$V_2\left[\frac{1}{R_2}+\frac{1}{R_3}\right]-V_s\frac{1}{R_2}=0$$

$$V_2=\frac{V_s}{R_2}\left(R_2 \parallel R_3\right)$$

$$V_2=V_s\left[\frac{R_3}{R_2+R_3}\right]$$

$$V_o=V_2\left(\frac{R_6(R_8+R_7)}{R_7(R_6+R_5)}\right)-V_1\frac{R_8}{R_7}$$

$$=V_2\left[\frac{10\mathrm{M}\left(4\mathrm{M}+2\mathrm{M}\right)}{2\mathrm{M}\left(10\mathrm{M}+5\mathrm{M}\right)}\right]-V_1\left[\frac{4\mathrm{M}}{2\mathrm{M}}\right]$$

$$=-2\left(V_2-V_1\right)$$

$$=-2V_s\left(\left[\frac{R_3}{R_2+R_3}\right]-\left[\frac{R_1}{R_1+R_t}\right]\right)$$

$$=-4.5+9\left(\frac{10k}{10k+10k\exp\left[3950\left(\frac{1}{T}-\frac{1}{298}\right)\right]}\right)$$

The final output voltage is related to the thermistor resistance by the equation of Vo.

The temperature circuit was also designed to be minimized onto a PCB, however, there were some constraints on the size of the board and ability to be somewhat flexible such as the Bandage thermometer discussed in Chapter 2. The circuit needs to be very small such as a bandage that can fit on the forehead and be able to be embedded inside a headband. Also, the circuit needs to be double-sided with the thermistor one-side, facing the skin, and the rest of the components facing the environment. This ensures that the aluminum does not short circuit any components. Flexible materials that are used for PCB fabrication, however, were not available. Even with these constraints, a prototype design, however, was still implemented in CadSoft Eagle as shown in Figure 25. The dimensions of the circuit are 4mm x 1mm, small enough for a person to wear on the forehead.

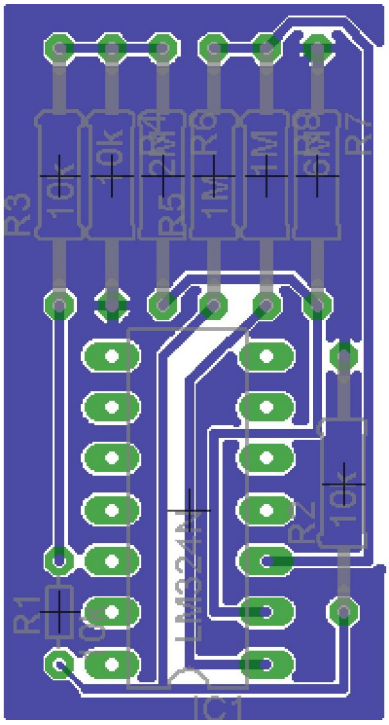

Figure 25. PCB design in CadSoft Eagle for the temperature circuit

4.2: Design of the EOG system

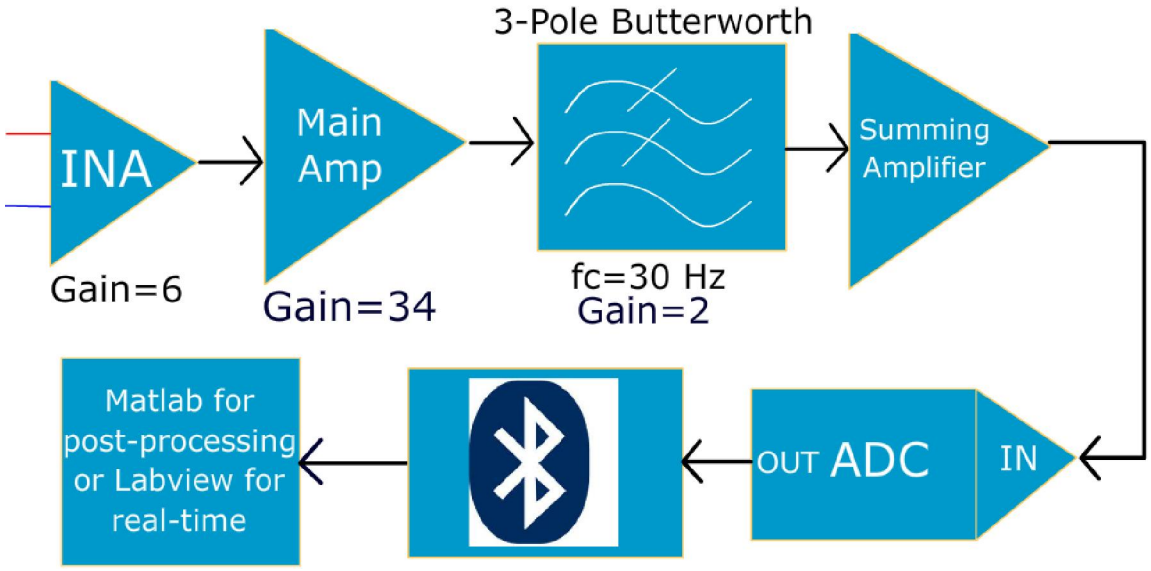

Figure 26. EOG Block diagram

The EOG system is a parallel architecture that has two paths, one is horizontal and the other is vertical; the circuit topology of both are exactly the same as shown in Figure 26. The EOG will consist of three total electrodes – these are re-usable electrodes that are 99% pure silver (Ag) and covered with a heavy gold-plate (see Figure 27).

Figure 27. The electrode that will be used in the EOG for NIHMS[11]

For this prototype, the embedded electrodes within the headband will not be implemented and the electrodes will be attached manually for testing purposes. The procedure for

[11] http://img.alibaba.com/photo/10948731/Gold_Eeg_Large_Electrode_Cup.jpg

attaching the electrodes is as follows: first, the patient uses alcohol pads around the area where the electrode will be attached to remove any particles that may add impedance; second, an adhesive paste is put in the electrode that is intended to minimize skin impedance; last, the electrode is placed on the area of interest and medical tape is used to fixate it. The electrodes borrowed for this project had end-connectors that required an adapter to connect. To improvise, a paper-clip was inserted to the end-connector with a wire connected to the paper clip and electrical tape used to bind these together. The configuration for connecting the electrodes was shown before in Figure 18 and Figure 20, where the reference electrode is attached to the mastoid bone located behind the earlobe.

The differential signals of these electrodes will then be connected to an instrumental amplifier, particularly, the INA114 from Texas Instruments. This was chosen particularly for the low input voltage offset, which offers very high input impedance. The gain of the instrumentation amplifier is 6, followed by a non-inverting amplifier with a gain of 34. After the main amplifier, the signal goes through a 3-pole Butterworth filter at a cutoff frequency of 30 Hz. The Butterworth topology was chosen due the flatness in the passband, however, due to the very slow roll-off, some high frequency components still exist after this stage. The input signal range to the microcontroller is 0-5 V, therefore, the signal needs to be shifted up. To do this, a non-inverting summing amplifier is used with an offset of about 2.5 V. The output of this signal is fed into the microcontroller and then wirelessly via Bluetooth to a processor. The exact circuit topology is shown in Figure 28.

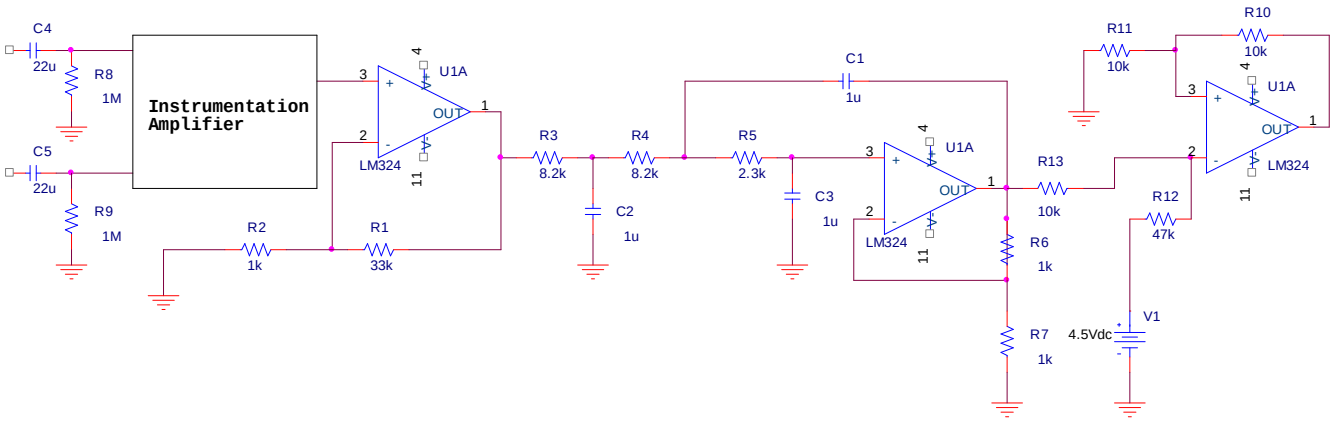

Figure 28. EOG circuit topology for both horizontal and vertical signals

In this circuit, coupling capacitors were used to eliminate dc offsets before the instrumentation amplifier. These are basically high-pass filters with a cutoff frequency of around .045 Hz; this still does not filter the saccadic amplitudes that we are interested in. The supply for all op-amps was +4.5 V and -4.5 V and all the capacitors used were 1uF.

CHAPTER 5: RESULTS AND DISCUSSION

5.1: Results for Temperature

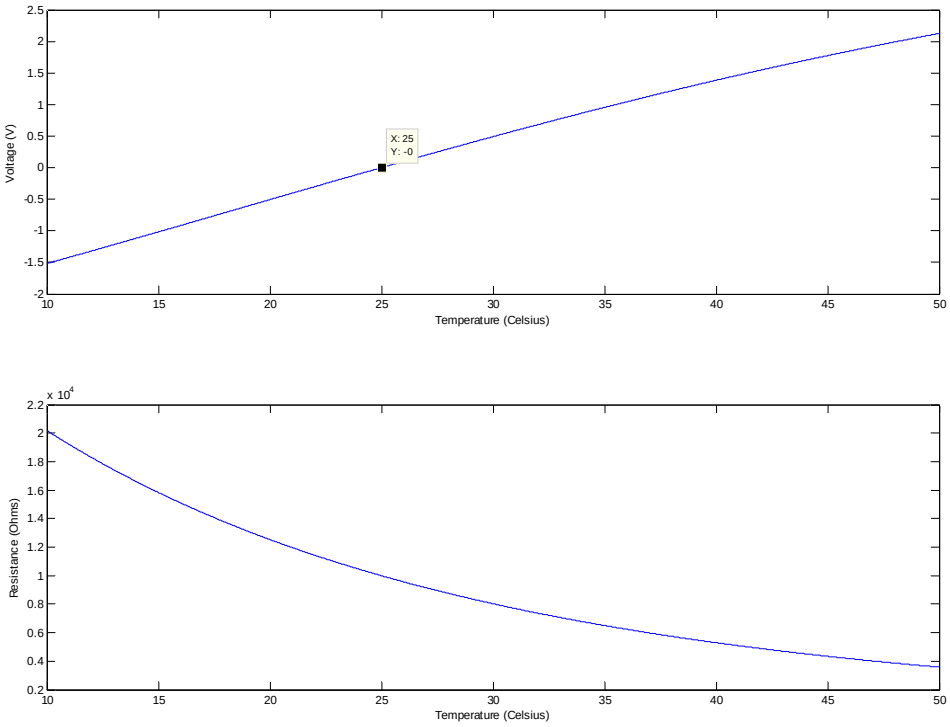

Figure 29. Plots of Voltage vs. Temperature and Resistance vs. Temperature respectively in Matlab

Graphing the relationship between voltage and temperature yields the above graph, Figure 29. It is shown that the relationship is mostly linear and the voltage is positive after 25° C. Therefore, the range is limited to 25-50° C because the input signal range for the microcontroller is 0-5 V. This is just fine because the core temperature should be around 37° C. The resolution of the temperature values can be recorded to 2 decimal places because the microcontroller is able to read up two 2 decimal places for the voltage. The values obtained from the temperature circuit were compared with a real digital thermometer and calibrated with a constant. The values are shown in Table 1.

Table 1. Calibration results of the temperature circuit versus a real digital thermometer

Temperature from Digital Thermometer (˚C)	Corresponding Temperature from Circuit (˚C)
32.01	32.01
33.09	33.31
32.23	32.23
32.76	33.09
32.55	32.66

These values do not reflect the core temperature, but the skin temperature on the surface of the head; this is due to the assumptions that were made earlier. In the future, another thermistor can be employed to measure the temperature of the insulator and calculate the ratio of the heat transfer coefficients. For this prototype, however, it is assumed that the skin temperature is 4° C from the core temperature.

5.2: Results from the EOG circuit:

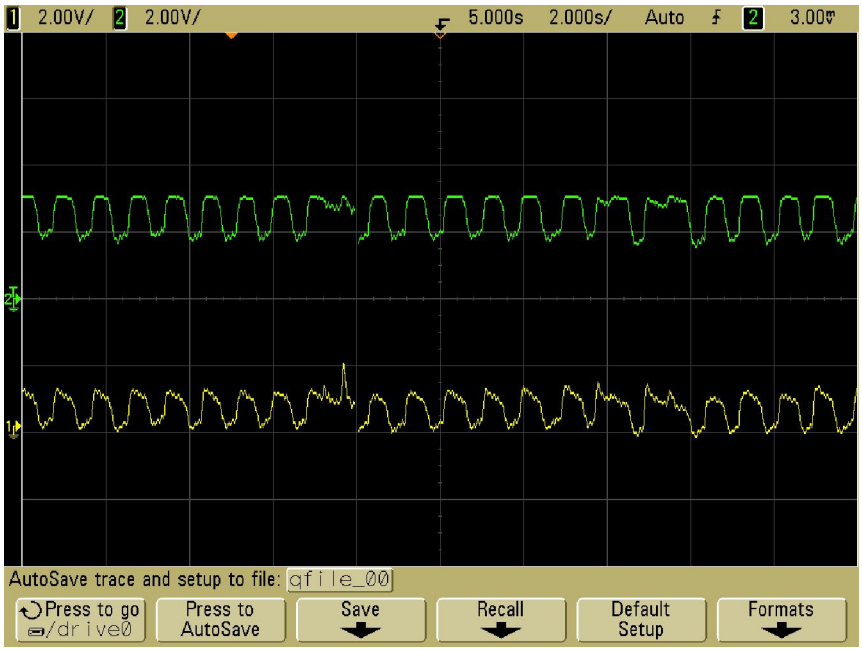

Figure 30. Horizontal saccades shown on the horizontal output (green) and the vertical output (yellow)

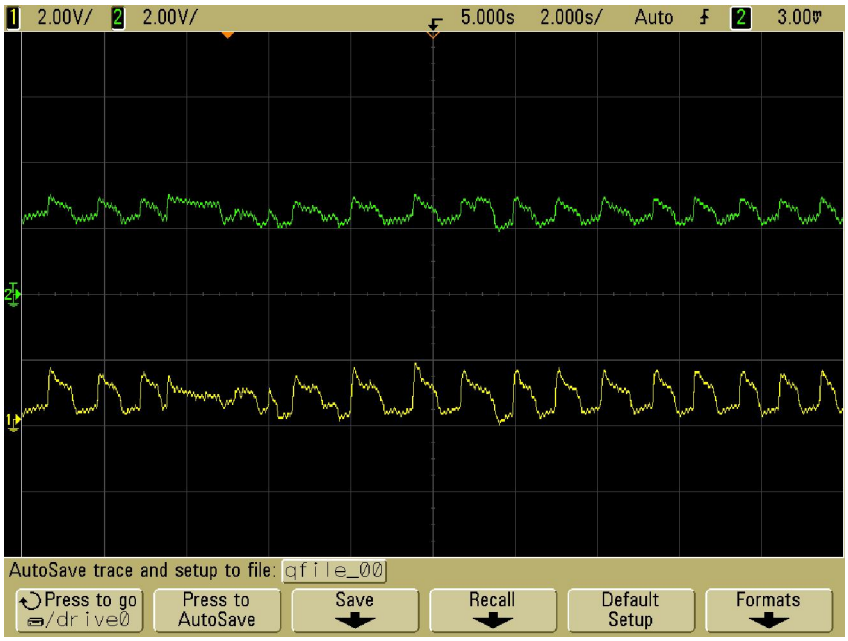

Figure 31. Vertical saccades shown on the horizontal output (green) and the vertical output (yellow)

Figure 30 and Figure 31 show the horizontal and vertical saccades respectively. The signal on the top (green) is the horizontal component while the signal below (yellow) is the vertical component. It is observed, then that in Figure 30, there are higher amplitudes in the horizontal component since the patient is performing horizontal saccades while we see a lower amplitude signal in Figure 31 because the patient is performing vertical saccades, which has a larger vertical component than horizontal.

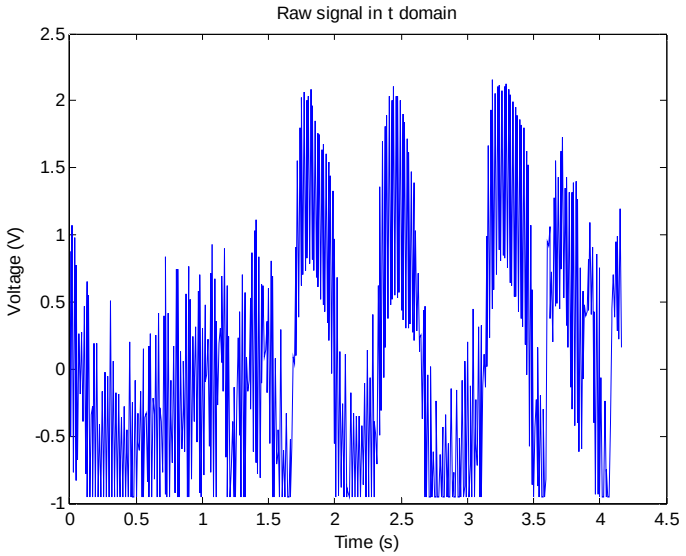

Figure 32. Raw EOG signal (vertical saccades) in time domain

After collecting many samples of horizontal and vertical saccades, the data was post-processed in Matlab. A raw sample for vertical saccades in time domain for 4.5 minutes is shown in Figure 32. The signal has many sources of noise, mostly high frequency components and some electromagnetic interference. The addition of coupling capacitors reduced the noise significantly. The data shown is after moving wires and the head, which shows that the prevalence of motion artifact is much attenuated. However, there are still many high frequency noise components present, so a Fourier transform must be done to see at what frequencies these components lie.

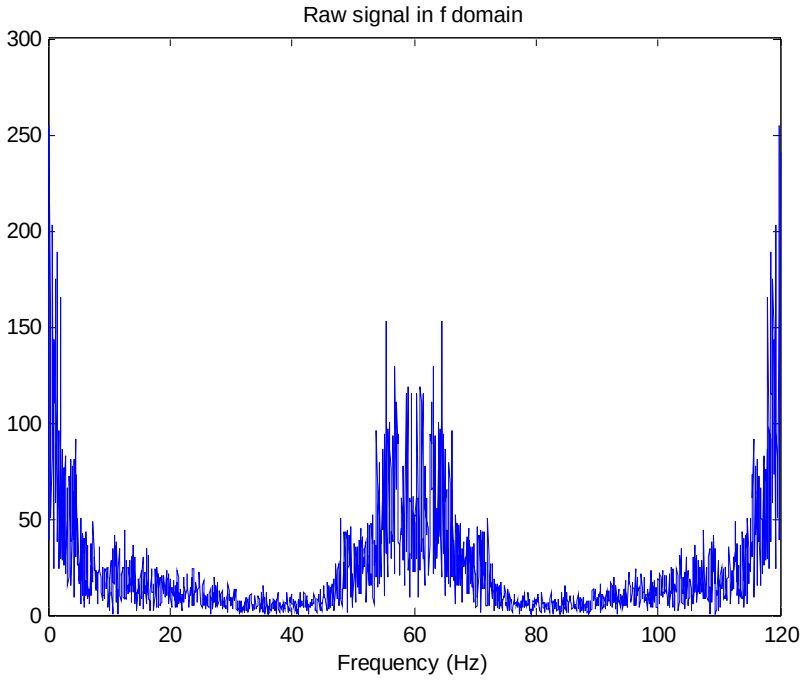

Figure 33. The raw EOG signal in frequency domain.

As seen from Figure 33, the noise depicted is mostly centered around 60 Hz, due to the fact that the power line also has a frequency of 60 Hz. A 120 Hz component is also seen, which is due to fluorescent lighting in the lab room that these results were collected. The original analog 3-pole Butterworth filter had a cutoff frequency of 30 Hz, which shows that the slow rolloff of the filter allowed many components to still pass. Therefore, digital filtering is required to set the components after 30 Hz to zero, which leads to Figure 34. Afterwards, the inverse fourier transform is taken and the result is shown in Figure 35.

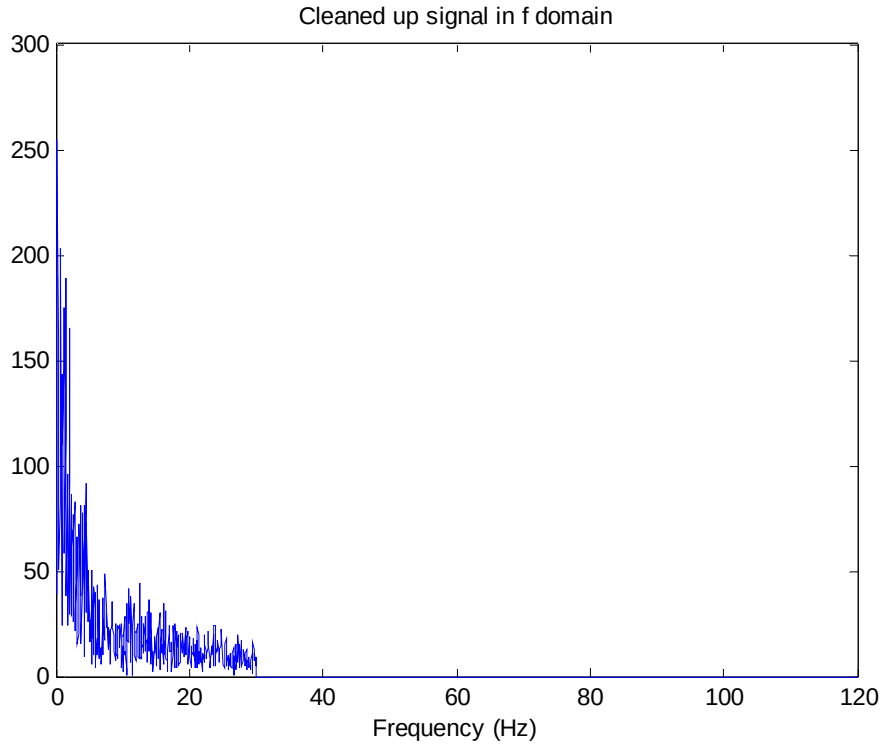

Figure 34. The processed EOG signal in frequency domain

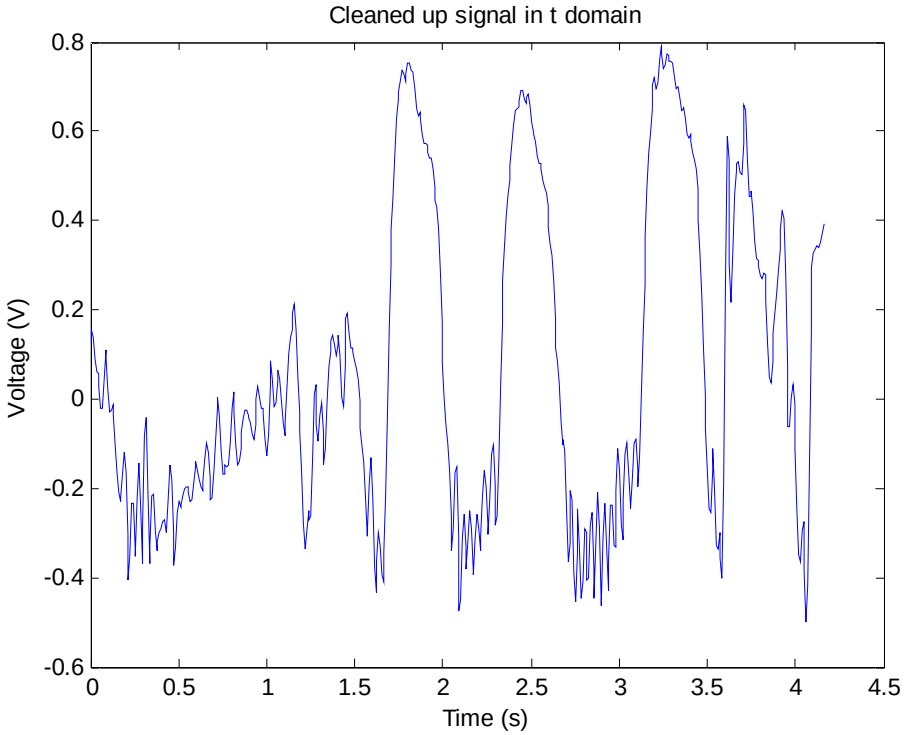

Figure 35. The processed EOG signal in time domain

The signal is much cleaner after digital filtering as shown. There are still some small noise components, however, present. From research, another method that is used to filter these noise components is called the Wavelet Transform. This is a joint time-frequency analysis (JTFA) method that informs at what time certain frequency components exist in the signal. The Wavelet transform in Matlab was used to assess this and a 'Haar' window was used. The Haar window was chosen because it most closely resembles a square wave, which is similar to the movements of the eye. This correlates with research. After a Discrete Wavelet transform of the signal, Figure 36 is the result. [5]

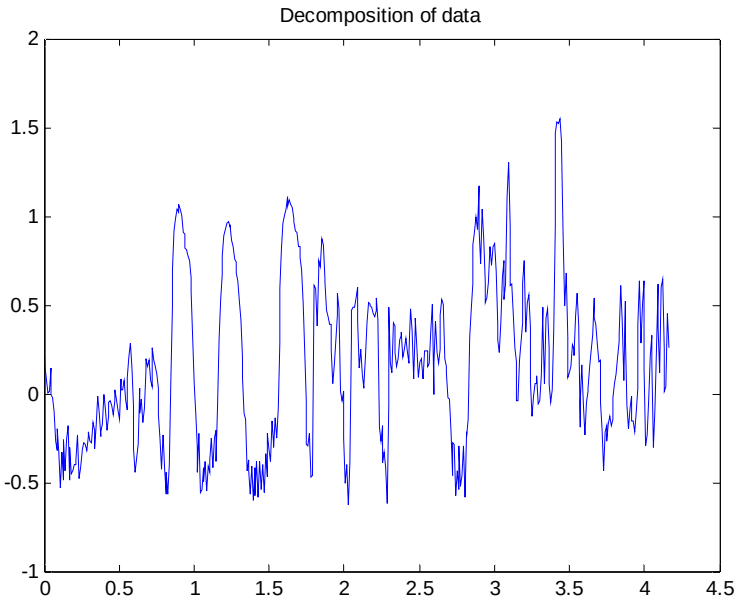

Figure 36. Discrete Wavelet Transform of the EOG signal

Just as the fourier transform, there are filter coefficients that relate the frequency components, in wavelet transform there are two coefficients that are computed: approximation and detail. In Matlab, this is how the dwt function is defined. After setting the detail coefficients to zero and performing an Inverse discrete wavelet transform, Figure 37 is the result. The difference between Figure 37 and Figure 35 is minimal, so it was determined that wavelet transform was not very useful in this prototype. Refer to Appendix B for Matlab codes. [5]

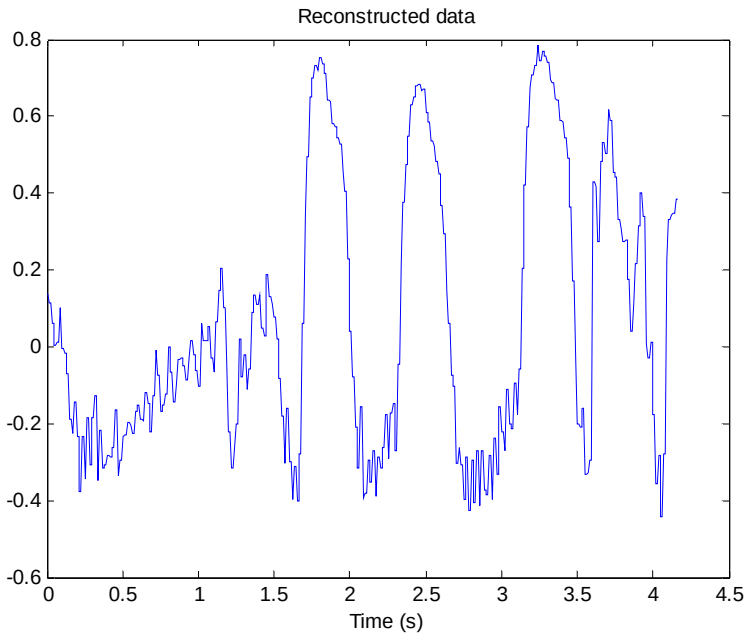

Figure 37. Inverse discrete wavelet transform of the EOG signal

After processing the signal, the Arden Ratio magnitude and Lp/Db ratio was computed as follows:

$$Arden\,Ratio\,Magnitude = \sqrt{(Vertical\ AR)^2 + (Horizontal\ AR)^2}$$
$$= \sqrt{(1.1738)^2 + (1.7491)^2}$$
$$\approx 2.1065\,or\,210.65\% > 150\%$$

$$LP\,/\,BL\,Magnitude = \sqrt{(Horizontal\ LP\,/\,BL)^2 + (Vertical\ LP\,/\,BL)^2}$$
$$= \sqrt{(1.1738)^2 + (1.164)^2}$$
$$\approx 1.6513\,or\,165.13\%$$

The results show that the EOG is normal and above 150%. The tests were performed on a 21-year old healthy university student. The Lp/Db ratio was also computed and is lower than the Arden Ratio as expected. The difference between these two ratios is .4552 or 45.52%. In this case, the EOG was normal, however, if it was abnormal, the diseases that it could diagnose are: Best's disease, Uveal Melanoma, Stagardt's disease, Amblyopia (lazy eye), and some other forms of macular degeneration (Refer to Section 3.3).

CHAPTER 6: CONCLUSIONS AND RECOMMENDATIONS

6.1: Project Summary

NIHMS was a project implemented to help people who are handicapped or people who need to be constantly monitored for vital signs. The aim of the project was to be non-invasive, wearable, portable, wireless, and real-time. The signals were to be sent wirelessly to a smart phone or a similar portable device in which a physician or the patient is able to receive diagnostic information. This system offers monitoring of an individual's vital signs and warns a physician before they become at a level where medical attention is necessary. This system also allows patients to monitor themselves instead of in a fixated environment such as the hospital.

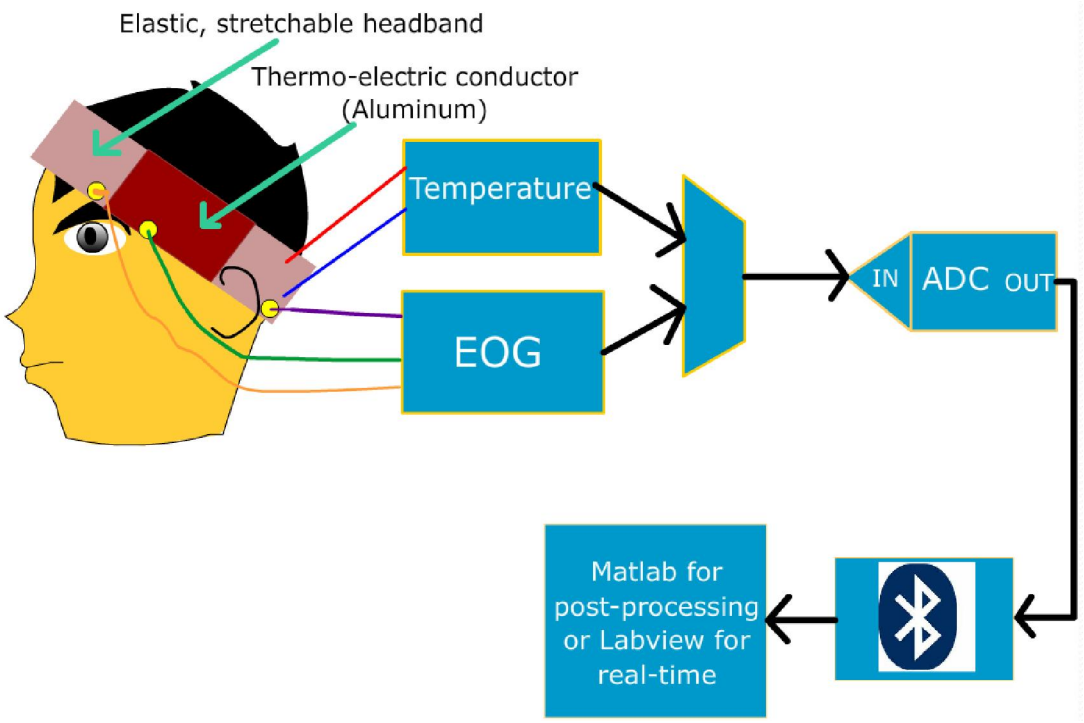

Figure 38. EOG and Temperature components of the NIHMS project aka the ET band

The prototype discussed in this paper consisted of two components of NIHMS: Temperature and EOG, also known as the ET band. The objective of the ET band was to determine the core temperature of the human body and the Arden Ratio from the EOG,

giving a diagnosis of the patient. The contraption starts as a headband that is a stretchable or adjustable belt-like material (Nylon). The ET band can be designed for left-side or right-side depending on the user's preference.

The temperature component of the headband is of a non-stretchable material because this is where the circuit is kept. Between the temperature circuit and the skin, a sheet of aluminum is kept that serves as a conductor to pass heat onto the thermistor. This measures the skin temperature which is near the core temperature.

Also, on three different points on the headband, there are three embedded electrodes. These points touch the top of the eye, the side of the eye, and the mastoid bone behind the ear. The horizontal and vertical saccadic amplitudes are then measured using the EOG circuit.

Both the signals from the temperature circuit and the EOG circuit are sent to the microcontroller, which uses a Bluetooth transmitter to send the signals wirelessly to a Bluetooth receiver. The Bluetooth receiver sends this to a computer or a smart phone for processing. In the processing, a prognosis is implemented based on the results received and the results of this prognosis is outputted to the user. The final block diagram is depicted in Figure 38.

6.2: Statement on Project Safety

One of the best qualities of NIHMS is that all the signals that are measured are non-invasive. Furthermore, the power source used is maximum 9 Volts, which is not potentially harmful to the user if any malfunction were to occur. The ET band is a wearable and comfortable device that conforms to any head size because of its adjustability. Entanglements of wires and possible disconnections are negated because NIHMS is wireless.

6.3: Challenges Faced and Recommendations for the future

Suggested improvements and problems with the EOG circuit:

There were numerous problems encountered during the NIHMS project and the development of the prototype ET band. First, EOG almost always accompanies EMG and EEG in some way or fashion. While EEG was suppressed, if a person were to jog or exercise, the EMG signal might increase where the signal-to-noise (SNR) ratio might be affected, where EMG would be considered as noise. Therefore, to suppress these signals, while maintaining a high SNR is difficult. This is the reason why algorithms like the Wavelet transform were considered. During the testing phase of this prototype, exercise was not regarded and therefore, a significantly higher than practical SNR was obtained.

Another problem was that different levels of illumination were not considered. All the calculations that were done were on a fixed illumination setting, but if the product were to be used in a different setting, the results could change. In real life, the environment has a variable illumination level, which could result in a different Lp/Db ratio for each of those levels. However, while the Lp/Db ratio changes, the Arden Ratio does not because it depends on the highest and lowest illumination levels only. Therefore, a recommended solution would be to develop a design that combines a photodiode to detect the level of illumination and then associate the corresponding Lp/Db ratio with this level. This way, the Lp/Db ratio can be correctly correlated with the Arden Ratio. For each level of illumination, there will be a different offset between the Arden Ratio and the Lp/Db ratio. The end result will be a feedback system. Another recommended solution would be to use comparators for different voltage ranges, each corresponding to a different illumination level.

An artifact which was not discussed earlier that might affect the results for calculating the Arden Ratio is blinking. Blinking causes sharp peaks to appear in the EOG signal and the amplitude of these peaks might be the maximum amplitude. Since the Arden Ratio is dependent on the maximum amplitude (Light peak), this might result in an overestimate. Therefore, there needs to be an algorithm to filter the blinking. A recommended

algorithm would be to take the derivative of a certain time interval; since the peaks are sharp, the slope will be very high, thus the derivative will be high as well. This way, the time of the blinks can be known and the signal can bet set to zero during that interval.

The last problem that was faced with the EOG was electromagnetic interference. While motion artifact and other sources of noise were mostly negated, the electrodes themselves still act like antennas and are still capable of receiving other signals. The recommended solution for this would be to use shielding. Since an elastic headband is being used, however, a metal mesh or a faraday cage is not possible. Therefore, the best alternative to shielding would be to spray the inside of the headband with a metallic ink which could consist of copper or nickel. Once this is dry, it will produce a continuous layer of conductive material, thus providing shielding.

Suggested Improvements and Problems with the Temperature circuit:

The problems faced with the temperature circuit were mainly the assumptions that were made in the beginning. That is, the temperature of the skin is the same as the temperature of the outside of the headband (the insulator). From results, it is clear that this is not true and the temperature of the headband then must be determined in order to calculate the core temperature accurately. A recommendation would be to use a second thermistor or an array of thermistors that is on the other side of the PCB. This way the temperature of the insulator can be determined and the core temperature can be calculated by finding the heat transfer coefficients.

Another problem was that the PCB which was designed was not flexible. While flexible PCBs are very expensive, because the shape of the head is curved, a PCB is also needed which can conform to the head shape.

6.4: Project Cost

The project costs for NIHMS discussed in this paper only include the ET band. Many of the parts required for this project were obtained from the faculty in McMaster University for free. These include resistors, capacitors, EEG paste, and electrodes. The savings for these free parts compared to their retail value is $132.92 CDN. Re-usable electrodes are necessary for consistency in the project and measurements. The remaining parts were purchased from Digikey. During the design phase of the project, there were many unnecessary purchases of parts; the instrumentation amplifiers in particular were purchased from 4 different models, in which the INA114 resulted in success. If this project were to be commercialized, the production costs would be less than $200 CDN. Overall, the cost of the project is shown in Table 2 where the actual costs paid totaled to $81.35 CDN, while the minimum costs required totaled to $192.45 CDN.

Table 2. Total Project Costs and Comparison between Minimum costs required and Actual Costs paid

Part	Quantity	Actual Costs Paid	Quantity	Minimum costs required
Instrumentation Amplifiers	4	$51.16	2	$16.60
Quad Op-Amps	4	$1.8	2	$0.90
NTC Thermistors	2	$5.34	1	$5.34
Resistors	34	Free!	34	$7.82
Capacitors	6	Free!	8	$3.00
Breadboard	1	$8.73	1	$8.73
Medical tape	1	$4.33	1	$4.33
Electrode paste	1	Free!	1	$11.78
Non-polarizable gold cup electrodes	3	Free!	3	$110.32
Total with tax		$81.35		$192.45

APPENDIX A: MATLAB CODE FOR VOLTAGE TO TEMPERATURE CONVERSION

```
clear all
close all

Vs=4.5;
To=298;
Beta=3950;
R25=10e3;
R1=10e3;
R2=10e3;
R3=10e3;
T=10:.01:50;
Rt=zeros(1,length(T));
for i=1:length(T)
    Rt(1,i)=R25*exp(Beta*((1/(T(1,i)+273))-(1/To)));
end
Vo=zeros(1,length(T));
for i=1:length(T)
    Vo(1,i)=2.5*Vs*(R3/(R2+R3))-2*Vs*(R1/(R1+Rt(1,i)));
end
subplot(2,1,1), plot(T,Vo),xlabel('Temperature
(Celsius)'),ylabel('Voltage (V)')
subplot(2,1,2), plot(T,Rt),ylabel('Resistance
(Ohms)'),xlabel('Temperature (Celsius)')
```

APPENDIX B: MATLAB CODES FOR FOURIER AND WAVELET TRANSFORMS IN PROCESSING OF EOG

Matlab Code for Fourier Transform:

```
clear all
close all
clc
load 'hnoise.txt'%saccades with noise in horizontal direction
load 'vnoise.txt'%saccades with noise in vertical direction

load 'hhsac.txt'%horizontal saccades in horziontal direction
load 'vhsac.txt'%horizontal saccades in vertical direction
load 'hvsac.txt'%vertical saccades in horizontal direction
load 'vvsac.txt'%vertical saccades in vertical direction
%
load 'hhsacdark.txt'%same thing but in dark
load 'vhsacdark.txt'
load 'hvsacdark.txt'
load 'vvsacdark.txt'
%
load 'hblink.txt'%blinking in horizontal direction
load 'vblink.txt'%blinking in vertical direction

offset=1;
hoffset=1.45;
voffset=1.14;
data=vnoise/1000-offset;
N=length(data);
T=1/120;
a=1;
b=500;
f=(1/T)*linspace(0,1,N);

lighth=hhsac/1e3-hoffset;
FFTlighth=fft(lighth);
FFTlighth(f(:)>30)=0;
lighth=abs(ifft(FFTlighth));

darkh=hhsacdark/1e3-hoffset;
FFTdarkh=fft(darkh);
FFTdarkh(f(:)>30)=0;
darkh=abs(ifft(FFTdarkh));

lightv=vvsac/1e3-voffset;
FFTlightv=fft(lightv);
FFTlightv(f(:)>30)=0;
lightv=abs(ifft(FFTlightv));

darkv=vvsacdark/1e3-voffset;
FFTdarkv=fft(darkv);
FFTdarkv(f(:)>30)=0;
darkv=abs(ifft(FFTdarkv));
```

```
ardenh=abs(max(lighth)/min(darkh));
ardenv=abs(max(lightv)/min(darkv));
ardenmag=sqrt(ardenh^2+ardenv^2);

FFTdata=fft(data);
t=linspace(0,T*N,length(data));
plot(t(a:b),data(a:b));title('Raw signal in t domain'),xlabel('Time
(s)'),ylabel('Voltage (V)')
figure, plot(f,abs(FFTdata)),title('Raw signal in f
domain'),xlabel('Frequency (Hz)')
FFTdata(f(:)>30)=0;
cleanedF=abs(FFTdata);
cleanedT=ifft(FFTdata);
figure, plot(f,cleanedF),title('Cleaned up signal in f
domain'),xlabel('Frequency (Hz)')
figure, plot(t(a:b),cleanedT(a:b)),title('Cleaned up signal in t
domain'),xlabel('Time (s)'),ylabel('Voltage (V)')
```

Matlab Code for Wavelet transform:

```
clear all
close all

load 'vnoise.txt'

offset=1;
hoffset=1.45;
voffset=1.14;
data=vnoise/1000-offset;
N=length(data);
T=1/120;
a=1;
b=500;
f=(1/T)*linspace(0,1,N);

T=1/120;
t=linspace(0,T*N,N);
N=length(data);
t=linspace(0,T*N,N);

[cA,cH] = dwt(data,'haar');
dec1d = [cA,cH];
cleanCH=idwt(cA,zeros(size(cH)),'Haar');
cleanCA=idwt(zeros(size(cA)),cH,'Haar');

figure, plot(t(a:b),dec1d(a:b)),title('Decomposition of data')
figure, plot(t(a:b),cleanCH(a:b)),title('Reconstructed data 1')
figure, plot(t(a:b),cleanCA(a:b)),title('Reconstructed data 2')
```

APPENDIX C: COMPLETE CIRCUIT ON BREADBOARD

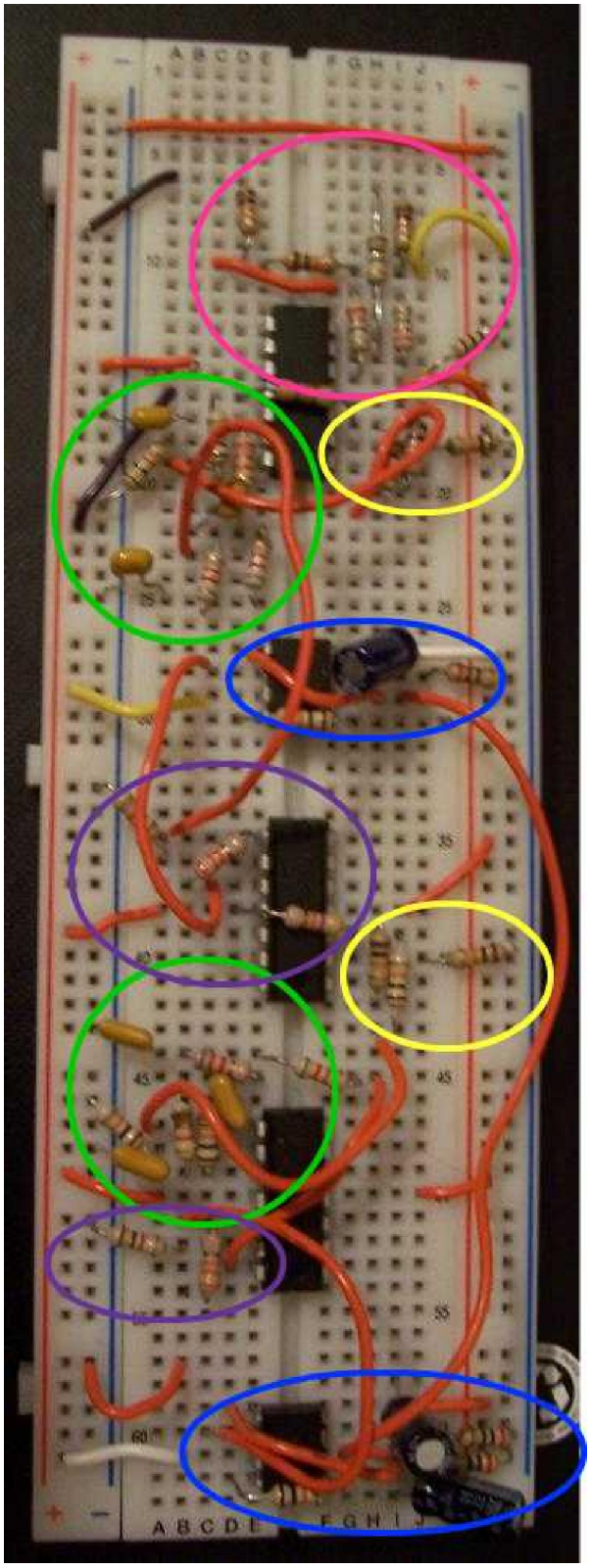

Legend:

- Instrumentation Amplifiers
- 3-Pole Butterworth filter
- Summing Amplifiers
- Non-inverting Main Amps
- Temperature circuit

APPENDIX D: GANTT CHARTS

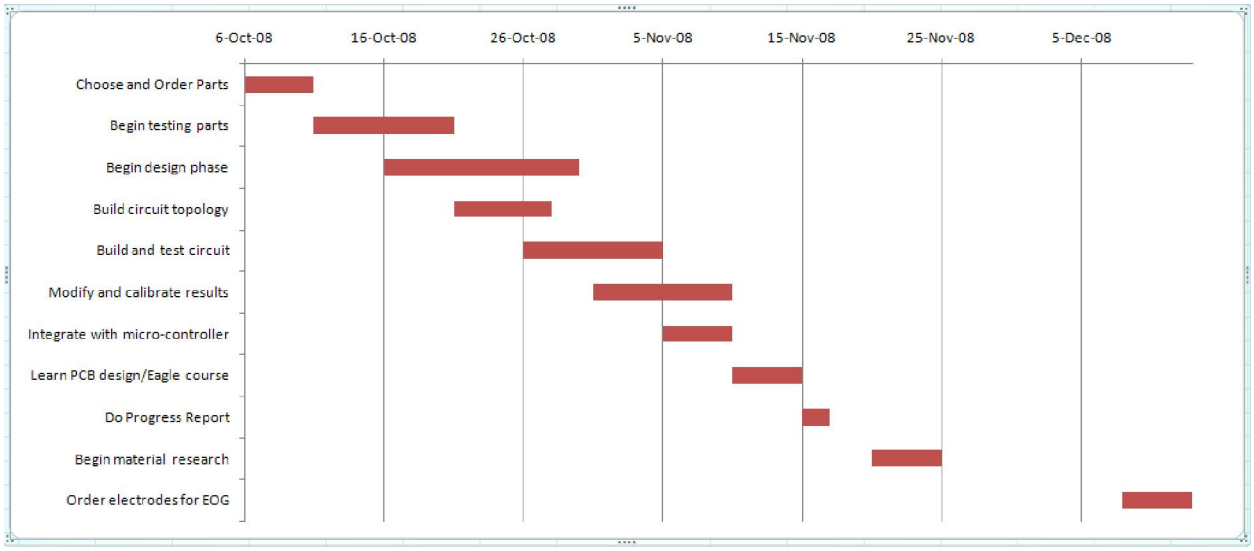

Figure 39. Gantt chart for 1st semester

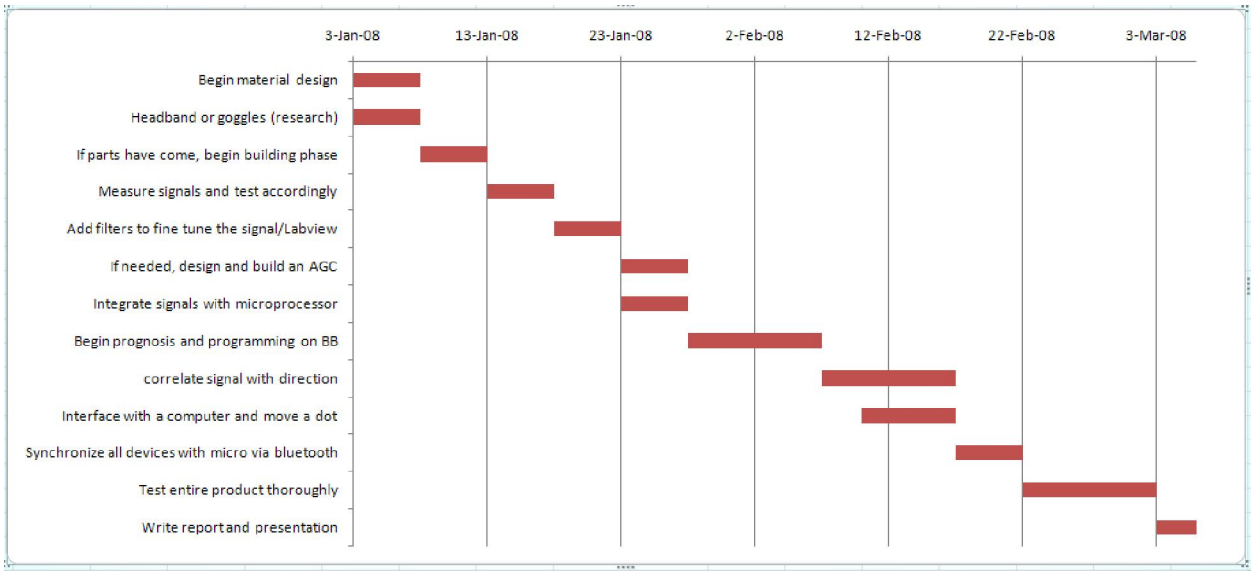

Figure 40. Gantt chart for 2nd semester

REFERENCES

[1] M. Brown, M. Marmor, Vaegan, E. Zrenner, M. Brigell and M. Bach. (2006, November 16, 2006). ISCEV standard for clinical electro-oculography (EOG) 2006. Springer Science+Business Media Available: http://www.pubmedcentral.nih.gov.libaccess.lib.mcmaster.ca/articlerender.fcgi?artid=1820752

[2] J. Charles, "Neural Interfaces Link the Mind and the Machine [Industry Trends]," Computer, vol. 32, pp. 16-18, 1999.

[3] D. Creel, "Clinical Electrophysiology," December 3, 2003. 2003. <http://webvision.umh.es.libaccess.lib.mcmaster.ca/webvision/ClinicalERG.html>

[4] I. G. Finvers, J. W. Haslett and G. Jullien, "Wireless temporal artery bandage thermometer," Biomedical Circuits and Systems Conference, 2006. BioCAS 2006. IEEE, pp. 166-169, 2006.

[5] C. K. Ho and M. Sasaki, "Brain-wave bio potentials based mobile robot control: wavelet-neural network pattern recognition approach," Systems, Man, and Cybernetics, 2001 IEEE International Conference on, vol. 1, pp. 322-328 vol.1, 2001.

[6] J. A. Kistemaker, E. A. D. Hartog and H. A. M. Daanen, "Reliability of an infrared forehead skin thermometer for core temperature measurements," Journal of Medical Engineering & Technology, vol. 30, pp. 252, 2006.

[7] S. Kodagoda, E. A. S. Hemachandra, P. A. A. R. Pannipitiya, L. S. Bartholomeuz and A. A. Pasqual, "Minimal Invasive Headband for Brain Computer Interfacing and Analysis," Information and Automation, 2006. ICIA 2006. International Conference on, pp. 109-114, 2006.

[8] H. S. Lusted and R. B. Knap. Controlling computers with neural signals. Available: http://www.absoluterealtime.com.libaccess.lib.mcmaster.ca/resume/SciAmBioCtl.pdf

[9] M. Modarreszadeh and R. N. Schmidt, "Wireless, 32-channel, EEG and epilepsy monitoring system," Engineering in Medicine and Biology Society, 1997. Proceedings of the 19th Annual International Conference of the IEEE, vol. 3, pp. 1157-1160 vol.3, 1997.

[10] M. S. Panse and S. K. Kulkarni, "Application of digital signal processing in ophthalmic research: a new horizon in biomedical engineering," Engineering in Medicine and Biology Society, 1995 and 14th Conference of the Biomedical Engineering Society of India. an International Meeting, Proceedings of the First Regional Conference. , IEEE, pp. 2/88, 1995.

[11] F. Pompei and M. Pompei, "Non-invasive temporal artery thermometry: Physics, physiology, and clinical accuracy," in Thermosense XXVI, 2004, pp. 61-67.

[12] Stephen Meredith. Measurement of eye movement using electro oculography. Available: http://ee.ucd.ie.libaccess.lib.mcmaster.ca/~smeredith/EOG_index.html

[13] C. S. L. Tsui, Pei Jia, J. Q. Gan, Huosheng Hu and Kui Yuan, "EMG-based hands-free wheelchair control with EOG attention shift detection," Robotics and Biomimetics, 2007. ROBIO 2007. IEEE International Conference on, pp. 1266-1271, 2007.

[14] Zhao Lv, Xiaopei Wu, Mi Li and Chao Zhang, "Implementation of the EOG-Based Human Computer Interface System," Bioinformatics and Biomedical Engineering, 2008. ICBBE 2008. the 2nd International Conference on, pp. 2188-2191, 2008.

VITA

NAME:	Aiyush Bansal
PLACE OF BIRTH:	Dehradun, India
YEAR OF BIRTH:	1987
SECONDARY EDUCATION:	Mount Pleasant High School (2003- 2005) Cypress Creek High School (2001-2003)
HONOURS and AWARDS:	McMaster Entrance Honor Award Michigan Merit Scholarship Award

1st place, Engineering Competition, University of Michigan Summer Engineering Program

2nd place, Robot Ramble Contest, 2005 Regional Science Olympiad (23 competing schools)

2nd place, Physics Lab, 2005 Regional Science Olympiad (23 competing schools)

2nd place, 2005 Quiz Bowl Competition (Inter-school competition)

2nd place, Brazilian Jiu-Jitsu competition, Regional, Houston, TX